

Synthesis and Ethylene Polymerization Capability of Metallocene-like Imido Titanium Dialkyl Compounds and Their Reactions with AlⁱBu₃

Paul D. Bolton,[†] Nico Adams,[†] Eric Clot,[‡] Andrew R. Cowley,[†] Paul J. Wilson,[§] Martin Schröder,[§] and Philip Mountford^{*,†}

Chemistry Research Laboratory, University of Oxford, Mansfield Road, Oxford OX1 3TA, U.K.,
Laboratoire de Structure et Dynamique des Systèmes Moléculaires et Solides (UMR 5636 CNRS-UM2),
Institut Charles Gerhardt, cc 14, Université Montpellier 2, 34095 Montpellier Cedex 5, France, and
School of Chemistry, University of Nottingham, University Park, Nottingham NG7 2RD, U.K.

Received July 7, 2006

A series of alkyl- and aryl-imido titanium dialkyl compounds Ti(NⁱBu)(Me₃[9]aneN₃)R₂ (R = Me (**1**), CH₂SiMe₃ (**3**), CH₂ⁱBu (**4**), CH₂Ph (**5**)), Ti(NR)(Me₃[9]aneN₃)Me₂ (R = ⁱPr (**6**), Ph (**7**), 3,5-C₆H₃(CF₃)₂ (**8**), 2,6-C₆H₃ⁱPr₂ (**9**), 2-C₆H₄CF₃ (**10**), 2-C₆H₄ⁱBu (**11**)), and Ti(NR)(Me₃[9]aneN₃)(CH₂SiMe₃)₂ (R = ⁱPr (**12**), Ar^F (**13**)) were prepared and crystallographically characterized in the case of **1**, **6–9**, and **11** (Me₃[9]aneN₃ = 1,4,7-trimethyl triazacyclononane; Ar^F = C₆F₅). These compounds, isolobal with the titanocenes Cp₂TiR₂, were thermally stable at elevated temperatures except for **4**. Reaction of **7** with [Ph₃C][BAR^F₄] (TB) and diisopropylcarbodiimide in CH₂Cl₂ gave the Ti–Me insertion product [Ti(NPh)(Me₃[9]aneN₃){MeC(NⁱPr)₂}] [BAR^F₄] (**15-BAR^F₄**). The corresponding reaction of **7** in the absence of organic substrate gave [Ti₂(μ-NPh)₂(Me₃[9]aneN₃)₂Cl₂] [BAR^F₄]₂ via a solvent activation reaction. The room-temperature ethylene polymerization capabilities of the dialkyl compounds were evaluated using TB cocatalyst in the presence of AlⁱBu₃ (TIBA). Among the dimethyl precatalysts, only the systems **1** and **11**, with the bulkiest imido groups, showed high productivities (6230 and 1210 kg mol⁻¹ h⁻¹ bar⁻¹, respectively). The productivities of the other *tert*-butyl imido precatalysts **3** and **4** (130 and 120 kg mol⁻¹ h⁻¹ bar⁻¹, respectively) were substantially lower than that of **1**. The catalyst system **1**/TIBA (2500 equiv, no added TB) was also active for ethylene polymerization (225 kg mol⁻¹ h⁻¹ bar⁻¹). The less productive imido dialkyl precatalysts all formed complex mixtures on exposure to TIBA. The polyethylenes produced with **1**, **3**, and **5–11** generally had *M*_w/*M*_n values in the range 2.6–3.0. The PE formed with **1**/TB/TIBA was terminated only by methyl end groups, consistent with chain transfer to TIBA followed by subsequent β-H transfer by the resultant titanium isobutyl cation. The alkyl cations [Ti(NⁱBu)(Me₃[9]aneN₃)R]⁺ (R = Me or CH₂SiMe₃) reacted rapidly with TIBA in C₆D₅Br at –30 °C, forming isobutene. DFT calculations found that TIBA adducts of the model methyl cation [Ti(NMe)(H₃[9]aneN₃)Me]⁺ were energetically favorable by ca. –80 to –110 kJ mol⁻¹. Whereas **1** alone or with AlMe₃ present has been shown to form only Ph₃CMe on reaction with [Ph₃C]⁺, 1:1 mixtures of **1** and TIBA gave Ph₃CH as the only trityl-containing product, suggesting a key role for transient [AlⁱBu₂]⁺ in the activation process for these catalysts. Overall, the imido group in the Ti(NR)(Me₃[9]aneN₃)Me₂/TB/TIBA catalysts systems appears to have two roles: to stabilize the dialkyl precatalyst toward degradation by the TIBA itself prior to activation, and to inhibit the formation of catalytically inactive hetero- or homo-bimetallic complexes.

Introduction

The development of nonmetallocene, transition metal olefin polymerization catalysts continues to be an area of considerable academic and industrial activity.^{1–8} Complexes of a wide range of heteroatom-donor supporting ligands have been prepared and

assessed, including transition metal imido compounds, L_nM(NR)_mX₂ (L_n = additional ligand or ligand set; X = alkyl or halide typically).⁸ The formally dianionic imido ligand [NR]²⁻ is isolobal with cyclopentadienide,^{9–12} a conceptual feature that has been used in the design of catalysts containing these N-donor groups. Group 6 bis(imido) and group 5 cyclopentadienyl-imido catalysts of the type M(NR)₂X₂ and CpM(NR)X₂, respectively,

* Corresponding author. E-mail: philip.mountford@chem.ox.ac.uk.

[†] University of Oxford.

[‡] Université Montpellier 2.

[§] University of Nottingham.

(1) Britovsek, G. J. P.; Gibson, V. C.; Wass, D. F. *Angew. Chem., Int. Ed.* **1999**, *38*, 429.

(2) Ittel, S. D.; Johnson, L. K.; Brookhart, M. *Chem. Rev.* **2000**, *100*, 1169.

(3) Piers, W. E.; Emslie, D. J. H. *Coord. Chem. Rev.* **2002**, *233–234*, 131.

(4) Gibson, V. C.; Spitzmesser, S. K. *Chem. Rev.* **2003**, *103*, 283.

(5) Suzuki, Y.; Terao, H.; Fujita, T. *Bull. Chem. Soc. Jpn.* **2003**, *76*, 1493.

(6) Mitani, M.; Saito, J.; Ishii, S.; Nakayama, Y.; Makio, H.; Matsukawa, N.; Matsui, S.; Mohri, J.; Furuyama, R.; Terao, H.; Bando, H.; H., T.; Fujita, T. *Chem. Rec.* **2004**, *4*, 137.

(7) Stephan, D. W. *Organometallics* **2005**, *24*, 2548.

(8) Bolton, P. D.; Mountford, P. *Adv. Synth. Catal.* **2005**, *347*, 355.

(9) Williams, D. S.; Schofield, M. H.; Anhaus, J. T.; Schrock, R. R. *J. Am. Chem. Soc.* **1990**, *112*, 6728.

(10) Glueck, D. S.; Green, J. C.; Michelman, R. I.; Wright, I. N. *Organometallics* **1992**, *11*, 4221.

(11) Williams, D. S.; Schofield, M. H.; Schrock, R. R. *Organometallics* **1993**, *12*, 4560.

(12) Gibson, V. C. *J. Chem. Soc., Dalton Trans.* **1994**, 1607.

have been assessed as isolobal analogues of the ubiquitous group 4 metallocene family.^{13–16} We have extended this approach by combining imido titanium¹⁷ fragments with neutral, six-electron donor ligands such as Me₃[9]aneN₃ (1,4,7-trimethyltriazacyclononane),^{18–23} tris(pyrazolyl)methanes,^{24,25} triazacyclohexanes,^{23,26} and others.^{18,27} Since both the dianionic NR²⁻ and conical *fac*-N₃ ligands²⁸ are isolobal with C₅H₅⁻, the compounds Ti(NR)(*fac*-N₃)X₂ (X = halide or alkyl) are also isolobal analogues of the group 4 metallocenes Cp₂MCl₂. We have also described detailed studies of the electronic structures of Ti(NR)(Me₃[9]aneN₃)X₂, certain well-defined monoalkyl cations [Ti(N^tBu)(Me₃[9]aneN₃)R]⁺ (R = Me or CH₂SiMe₃), and their relationships to the isolobal bis(cyclopentadienyl)-titanium systems.²² The alkyl cations were prepared by reaction of [Ph₃C][BAR^F₄] (TB, Ar^F = C₆F₅) with the corresponding dialkyls, the syntheses of which are reported for the first time here.

Of the Ti(NR)(*fac*-N₃)Cl₂/MAO catalyst systems studied (MAO = methylaluminoxane), those with Me₃[9]aneN₃ and tris-(3,5-dimethylpyrazolyl)methane co-ligands gave the best productivities and molecular weight distributions. Furthermore, only compounds with bulky imido R-substituents (e.g., R = ^tBu, adamantyl, 2-C₆H₄^tBu) afforded highly productive catalysts, especially under more commercially relevant conditions.^{20,23,25} We recently found analogous structure–productivity trends in an isostructural series of vanadium(IV) catalyst systems V(NR)-{HC(Me₂pz)₃}Cl₂/MAO, implying that adequate steric protection of the Ti=NR bond is a prerequisite for highly active systems.²⁹

MAO is one of the most widely used activators in Ziegler–Natta catalysis, especially with regard to metallocene systems.^{30–34}

It fulfills a dual role as both a precatalyst activator and impurity scavenger, and is typically used in a large Al:M ratio. The active species in Ziegler–Natta systems are cationic alkyl complexes of the type “[L_nM–R]⁺”.^{4,32–34} Typically, however, the MAOs used in these studies contain up to 20–30 wt % AlMe₃ (TMA), and the catalyst resting state in these instances is probably a bimetallic species of the type [L_nM(μ-R)₂AlR₂]⁺.^{35–44} Even this can be a simplistic view, with a range of homo- and hetero-bimetallic alkyl and alkyl-chloride species potentially being formed when dichloride precatalysts are activated with an excess of MAO.^{37,40,45} For example, the titanium species formed in the reactions of Cp₂TiCl₂ with an excess of MAO included Cp₂TiMe₂, Cp₂TiMeCl, [Cp₂TiMe(μ-Cl)Cp₂TiCl]⁺, [Cp₂TiMe(μ-Cl)Cp₂TiMe]⁺, [Cp₂TiMe(μ-Me)Cp₂TiMe]⁺, and [Cp₂Ti(μ-Me)₂AlMe₂]⁺.⁴⁰

As mentioned, we have recently reported the well-defined monoalkyl cations [Ti(N^tBu)(Me₃[9]aneN₃)R]⁺ (R = Me or CH₂SiMe₃) and some preliminary accounts of their reactions, including stoichiometric Ti–R bond insertion, Lewis base addition, and C–H bond and solvent activation processes.^{20–22} However, the methyl cation [Ti(N^tBu)(Me₃[9]aneN₃)Me]⁺ also formed the mono(μ-methyl)-bridged homobimetallic species [Ti₂(N^tBu)₂(Me₃[9]aneN₃)₂Me₂(μ-Me)]⁺ with excess Ti(N^tBu)-(Me₃[9]aneN₃)Me₂ (**1**)²² and the stable bis(μ-methyl)-bridged heterobimetallic [Ti(N^tBu)(Me₃[9]aneN₃)(μ-Me)₂AlMe₂]⁺ with TMA.²¹ The chloride cation [Ti(N^tBu)(Me₃[9]aneN₃)Cl]⁺ formed the homobimetallic species [Ti₂(N^tBu)₂(Me₃[9]aneN₃)₂Me₂(μ-Cl)]⁺ on reaction with **1**.²² These rather stable bimetallic complexes are analogues of the titanocenium and zirconocenium species identified in MAO-activated metallocene catalyst systems.^{40,45} Although we have no direct evidence for the presence of such species in the Ti(NR)(*fac*-N₃)Cl₂/MAO catalyst systems, it is not unlikely they could represent catalyst trapping and/or deactivation routes. The extent to which each species might form would likely depend on the imido substituents, which would in turn influence the overall structure–productivity relationships in these catalysts.

Preliminary experiments on the dialkyl compounds Ti(N^tBu)-(Me₃[9]aneN₃)R₂ (R = Me (**1**) or CH₂SiMe₃ (**3**)) as polymerization precatalysts were promising and suggested that they would offer a way to avoid MAO as an activator-scavenger.²⁰ Reaction of **3** with TB on the NMR tube scale followed by addition of C₂H₄ afforded a copious white precipitate of polyethylene (PE). Polymerization of ethylene with **1** using TB

(13) Chan, M. C. W.; Chew, K. C.; Dalby, C. I.; Gibson, V. C.; Kohlmann, A.; Little, I. R.; Reed, W. *Chem. Commun.* **1998**, 1673.

(14) Coles, M. P.; Dalby, C. I.; Gibson, V. C.; Little, I. R.; Marshall, E. L.; Ribeiro, da Costa, M. H.; Mastroianni, S. *J. Organomet. Chem.* **1999**, *591*, 78.

(15) Sato, Y.; Nakayama, Y.; Yasuda, H. *J. Appl. Polym. Sci.* **2005**, *97*, 1008.

(16) Coles, M. P.; Dalby, C. I.; Gibson, V. C.; Clegg, W.; Elsegood, M. R. *J. Chem. Soc., Chem. Commun.* **1995**, 1709.

(17) Hazari, N.; Mountford, P. *Acc. Chem. Res.* **2005**, *38*, 839.

(18) Wilson, P. J.; Blake, A. J.; Mountford, P.; Schröder, M. *Chem. Commun.* **1998**, 1007.

(19) Male, N. A. H.; Skinner, M. E. G.; Wilson, P. J.; Mountford, P.; Schröder, M. *New J. Chem.* **2000**, *24*, 575.

(20) Adams, N.; Arts, H. J.; Bolton, P. D.; Cowell, D.; Dubberley, S. R.; Friederichs, N.; Grant, C.; Kranenburg, M.; Sealey, A. J.; Wang, B.; Wilson, P. J.; Cowley, A. R.; Mountford, P.; Schröder, M. *Chem. Commun.* **2004**, 434.

(21) Bolton, P. D.; Clot, E.; Cowley, A. R.; Mountford, P. *Chem. Commun.* **2005**, 3313.

(22) Bolton, P. D.; Clot, E.; Adams, N.; Dubberley, S. R.; Cowley, A. R.; Mountford, P. *Organometallics* **2006**, *25*, 2806.

(23) Adams, N.; Arts, H. J.; Bolton, P. D.; Cowell, D.; Dubberley, S. R.; Friederichs, N.; Grant, C. M.; Kranenburg, M.; Sealey, A. J.; Wang, B.; Wilson, P. J.; Zuideveld, M. A.; Blake, A. J.; Schröder, M.; Mountford, P. *Organometallics* **2006**, *25*, 3888.

(24) Lawrence, S. C.; Skinner, M. E. G.; Green, J. C.; Mountford, P. *Chem. Commun.* **2001**, 705.

(25) Bigmore, H. R.; Dubberley, S. R.; Kranenburg, M.; Lawrence, S. C.; Sealey, A. J.; Selby, J. D.; Zuideveld, M.; Cowley, A. R.; Mountford, P. *Chem. Commun.* **2006**, 436.

(26) Wilson, P. J.; Blake, A. J.; Mountford, P.; Schröder, M. *J. Organomet. Chem.* **2000**, *600*, 71.

(27) Wilson, P. J.; Blake, A. J.; Mountford, P.; Schröder, M. *Inorg. Chim. Acta* **2003**, *345*, 44.

(28) Elian, M.; Chen, M. M. L.; Mingos, D. M. P.; Hoffmann, R. *Inorg. Chem.* **1976**, *15*, 1148.

(29) Bigmore, H. R.; Zuideveld, M.; Kowalczyk, R. M.; Cowley, A. R.; Kranenburg, M.; McInnes, E. J. L.; Mountford, P. *Inorg. Chem.* **2006**, *45*, 6411.

(30) Chen, E. Y.-X.; Marks, T. J. *Chem. Rev.* **2000**, *100*, 1391.

(31) Bochmann, M. *J. Chem. Soc., Dalton Trans.* **1996**, 255.

(32) Bochmann, M. *J. Organomet. Chem.* **2004**, *689*, 3982.

(33) Brintzinger, H. H.; Fischer, D.; Mülhaupt, R.; Rieger, B.; Waymouth, R. M. *Angew. Chem., Int. Ed. Engl.* **1995**, *34*, 1143.

(34) Kaminsky, W. *J. Chem. Soc., Dalton Trans.* **1998**, 1413.

(35) Bochmann, M.; Lancaster, S. J. *Angew. Chem., Int. Ed. Engl.* **1994**, *33*, 1634.

(36) Bochmann, M.; Lancaster, S. J. *J. Organomet. Chem.* **1995**, *497*, 55.

(37) Tritto, I.; Donetti, R.; Sacchi, M. C.; Locatelli, P.; Zannoni, G. *Macromolecules* **1997**, *30*, 1247.

(38) Vollmerhaus, R.; Rahim, M.; Tomaszewski, R.; Xin, S.; Taylor, N. J.; Collins, S. *Organometallics* **2000**, *19*, 2161.

(39) Zakharov, I. I.; Zakharov, V. A. *Macromol. Theory Simul.* **2002**, *11*, 352.

(40) Bryliakov, K. P.; Talsi, E. P.; Bochmann, M. *Organometallics* **2004**, *23*, 149.

(41) Schröder, L.; Brintzinger, H. H.; Babushkin, D. E.; Fischer, D.; Mülhaupt, R. *Organometallics* **2005**, *24*, 867.

(42) Bryliakov, K. P.; Babushkin, D. E.; Talsi, E. P.; Voskobynikov, A. Z.; Gritzko, H.; Schröder, L.; Damrau, H.-R. H.; Wieser, U.; Schaper, F.; Brintzinger, H. H. *Organometallics* **2005**, *24*, 894.

(43) Petros, R. A.; Norton, J. R. *Organometallics* **2005**, *23*, 5105.

(44) Eilertsen, J. L.; Støvneng, J. A.; Ystenes, M.; Rytter, E. *Inorg. Chem.* **2005**, *44*, 4843.

(45) Babushkin, D. E.; Semikolenova, N. V.; Zakharov, V. A.; Talsi, E. P. *Macromol. Chem. Phys.* **2000**, *201*, 558.

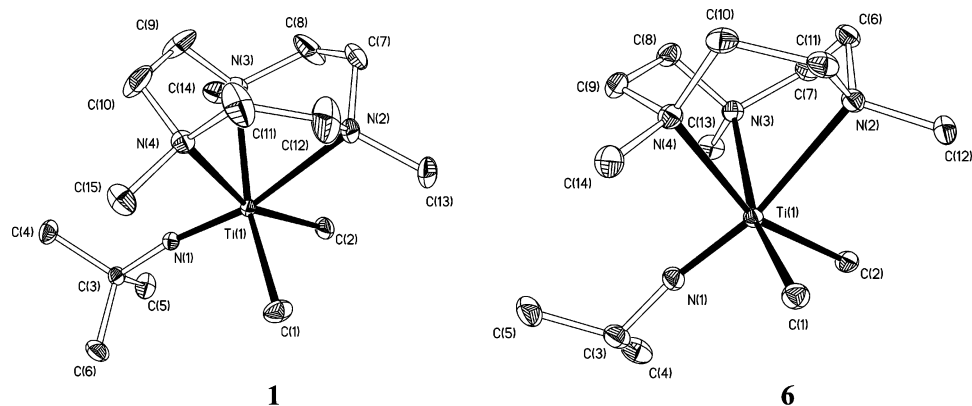


Figure 1. Displacement ellipsoid plots (20% probability) of alkyl imido compounds $\text{Ti}(\text{NR})(\text{Me}_3[9]\text{aneN}_3)\text{Me}_2$ ($\text{R} = \text{}^t\text{Bu}$ (**1**), $\text{}^i\text{Pr}$ (**6**)). H atoms are omitted.

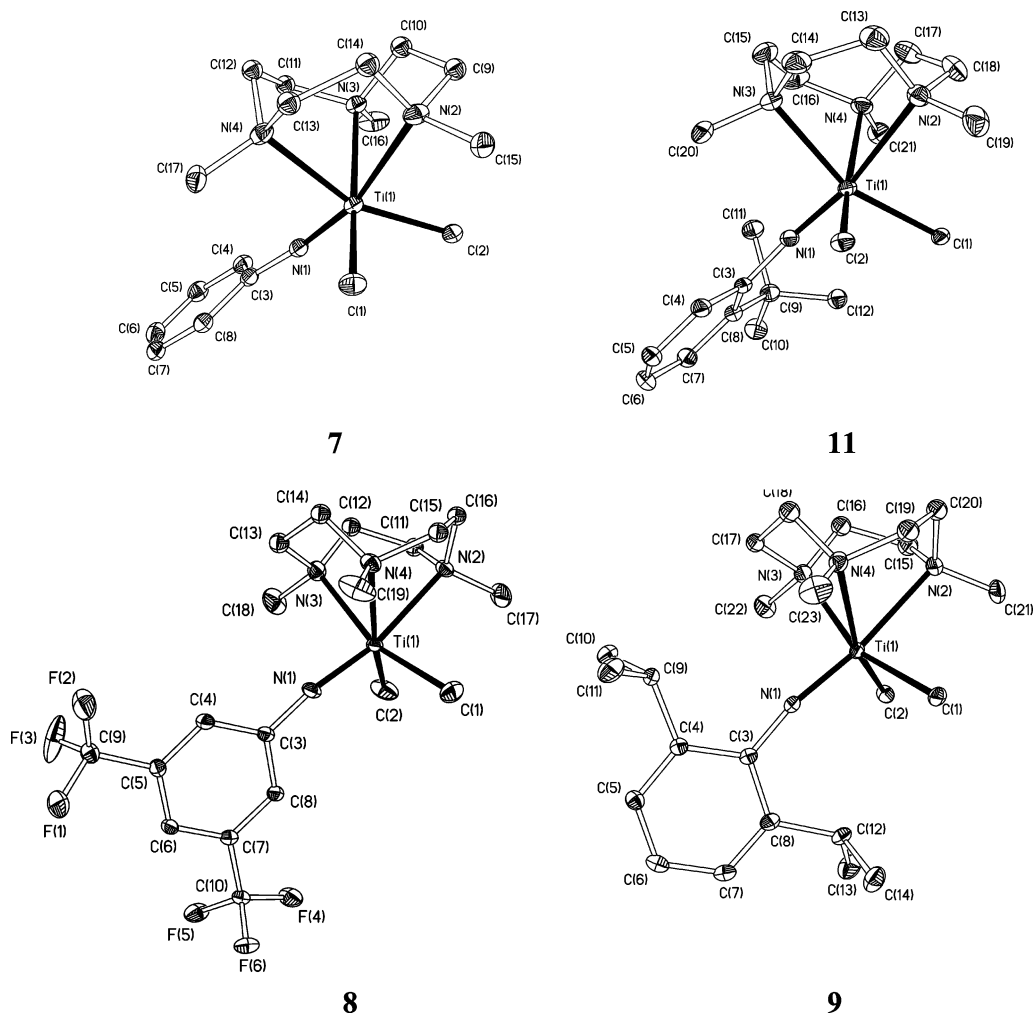


Figure 2. Displacement ellipsoid plots (20–25% probability) of the aryl imido compounds $\text{Ti}(\text{NAr})(\text{Me}_3[9]\text{aneN}_3)\text{Me}_2$ ($\text{Ar} = \text{Ph}$ (**7**), $\text{C}_6\text{H}_3(\text{CF}_3)_2$ (**8**), $2,6\text{-C}_6\text{H}_3\text{}^i\text{Pr}_2$ (**9**), $2\text{-C}_6\text{H}_4\text{}^t\text{Bu}$ (**11**)). H atoms are omitted.

straightforwardly gave pale yellow $\text{Ti}(\text{}^i\text{Pr})(\text{Me}_3[9]\text{aneN}_3)(\text{CH}_2\text{-SiMe}_3)_2$ (**12**). However, the corresponding reactions with $\text{Ti}(\text{NR})(\text{Me}_3[9]\text{aneN}_3)\text{Cl}_2$ ($\text{R} = \text{Ph}$ or $2,6\text{-C}_6\text{H}_3\text{}^i\text{Pr}_2$) were unsuccessful, while that with $\text{Ti}(\text{NAr}^{\text{F}})(\text{Me}_3[9]\text{aneN}_3)\text{Cl}_2$ gave $\text{Ti}(\text{NAr}^{\text{F}})(\text{Me}_3[9]\text{aneN}_3)(\text{CH}_2\text{SiMe}_3)_2$ (**13**) in only 8% yield. The X-ray structures of $\text{Ti}(\text{NR})(\text{Me}_3[9]\text{aneN}_3)\text{Me}_2$ ($\text{R} = \text{}^t\text{Bu}$ (**1**), $\text{}^i\text{Pr}$ (**6**), Ph (**7**), $3,5\text{-C}_6\text{H}_3(\text{CF}_3)_2$ (**8**), $2,6\text{-C}_6\text{H}_3\text{}^i\text{Pr}_2$ (**9**), and $2\text{-C}_6\text{H}_4\text{}^t\text{Bu}$ (**11**)) have been determined. Selected bond lengths and angles are listed in Table 1, and the molecular structures are shown in Figures 1 (compounds **1** and **6**) and 2 (compounds

7–9 and **11**). The crystals of **1** and **6** contained benzene of crystallization. Minor disorder of some of the macrocycle methylene groups was satisfactorily resolved (see Supporting Information). All of the complexes adopt approximately octahedral structures. The parent dichloride complexes $\text{Ti}(\text{NR})(\text{Me}_3[9]\text{aneN}_3)\text{Cl}_2$ ($\text{R} = \text{}^t\text{Bu}$, Ph , $2,6\text{-C}_6\text{H}_3\text{}^i\text{Pr}_2$)²³ have been crystallographically characterized previously. The dimethyls have features similar to the dichlorides, but the Ti–N distances for the macrocycle and the imido groups are slightly longer in each case as a result of the electron-releasing methyl ligands.

Table 1. Selected Bond Lengths (Å) and Angles (deg) for Ti(NR)(Me₃[9]aneN₃)Me₂ (R = ^tBu (**1**), ⁱPr (**6**), Ph (**7**), 3,5-C₆H₃(CF₃)₂ (**8**), 2,6-C₆H₃Pr₂ (**9**), and 2-C₆H₄Bu (**11**))

parameter	1	6	7	8	9	11
Ti(1)–N(1)	1.7180(18)	1.7190(18)	1.746(3)	1.751(2)	1.755(2)	1.7644(16)
Ti(1)–N(2)	2.463(2)	2.4784(18)	2.435(3)	2.409(2)	2.452(2)	2.4703(18)
Ti(1)–N(3)	2.335(2)	2.3594(17)	2.337(2)	2.316(2)	2.328(2)	2.3328(17)
Ti(1)–N(4)	2.334(2)	2.3259(17)	2.334(2)	2.312(2)	2.338(2)	2.3440(17)
Ti(1)–C(1)	2.205(3)	2.206(2)	2.186(4)	2.176(3)	2.240(2)	2.2118(18)
Ti(1)–C(2)	2.221(3)	2.211(2)	2.186(3)	2.172(3)	2.226(2)	2.2008(19)
N(1)–C(3)	1.438(3)	1.437(3)	1.377(4)	1.362(3)	1.380(3)	1.388(2)
<i>trans</i> influence (Å) ^a	0.128(3)	0.119(3)	0.098(4)	0.093(3)	0.124(3)	0.138(3)
	0.129(3)	0.153(3)	0.101(4)	0.097(3)	0.114(3)	0.126(3)
N(1)–Ti(1)–N(2)	167.30(8)	168.41(7)	165.94(10)	168.81(9)	172.50(8)	169.89(7)
N(1)–Ti(1)–N(3)	97.90(8)	99.38(8)	97.56(10)	95.87(10)	100.37(9)	97.73(7)
N(1)–Ti(1)–N(4)	96.91(8)	96.99(7)	93.97(11)	98.68(9)	101.50(8)	102.19(7)
N(1)–Ti(1)–Cl(1)	99.02(11)	97.85(9)	97.76(16)	98.22(18)	97.78(10)	94.63(8)
N(1)–Ti(1)–Cl(2)	98.59(11)	100.25(8)	98.10(14)	98.97(12)	98.34(10)	100.72(7)
Cl(1)–Ti(1)–Cl(2)	98.13(15)	96.24(9)	101.23(13)	95.89(13)	97.35(10)	97.03(8)
Ti(1)–N(1)–C(3)	171.52(16)	172.32(17)	169.3(2)	166.8(2)	168.97(17)	158.70(13)

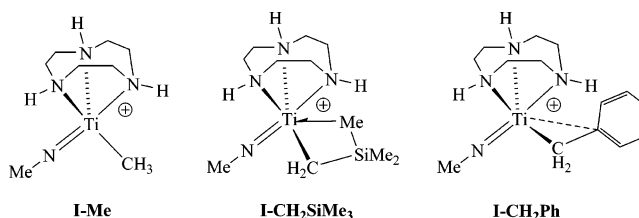
^a Defined as the difference between the Ti(1)–N(2) distance (i.e., *trans* to Ti=NR) and Ti(1)–N(3) and Ti(1)–N(4) distances.

The bonds to the imido ligands (Ti(1)–N(1)) are shorter for the alkyl imides **1** and **6** than for the aryl imides and slightly longer for the bulkier homologues among the latter group. These are common features of the structural chemistry of imido compounds.^{50,51} The significantly shorter Ti–N_{macrocycle} and Ti–Me distances in **8** are attributed to the electron-withdrawing *meta*-CF₃ groups. This is also reflected in the shorter N_{imide}–C_{ipso} distance in **8** (N(1)–C(3) = 1.362(3) Å) compared to those in the other aryl imides (range 1.377(4)–1.388(2) Å). All of the compounds show a lengthening of the Ti–N_{macrocycle} bond *trans* to the imide (Ti(1)–N(2)) relative to those in the *cis* positions (Ti(1)–N(3) and Ti(1)–N(4)). This *trans* labilizing influence of imido ligands is also well known.⁵² The largest *trans* influences (Table 1) are found for the alkyl imides **1** and **6** and for the more electron-donating aryl imides **9** and **11**.

Figure 2 shows that the N-aryl substituents in **7–9** and **11** adopt two types of orientation. The C₆H_xR_y (x + y = 5) ring carbons lie approximately within the molecular mirror planes in **8** and **9**, whereas in **7** and **11** the aryl rings are orientated perpendicular to this plane. In the case of **9**, analogous orientations of the aryl rings were found in the di-*ortho*-substituted chlorides Ti(N-2,6-C₆H₃R₂)(Me₃[9]aneN₃)Cl₂ (R = Me, ⁱPr);²³ for **11**, analogous orientations of the mono-*ortho*-substituted aryl rings were found in the vanadium chlorides V(N-2-C₆H₄R)(Me₃[9]aneN₃)Cl₂ (R = ^tBu, CF₃);²⁹ for **7**, an analogous orientation of the phenyl ring in Ti(NPh)(Me₃[9]aneN₃)Cl₂ was observed.²³ It appears that there is a common trend in the orientations of the aryl rings in complexes of the type M(NAr)(Me₃[9]aneN₃)X₂ (M = Ti, V; X = Cl, Me), which probably results from the minimization of intramolecular repulsions between the N–Ar and macrocycle N–Me groups.

Cationic Derivatives of Selected M(NR)(Me₃[9]aneN₃)R'₂ Complexes. In previous contributions we described the synthesis, electronic structures (using DFT),²² and, briefly, selected reactions²¹ of the *tert*-butyl imido alkyl cations [Ti(N^tBu)(Me₃[9]aneN₃)R]⁺ (R = Me or CH₂SiMe₃). While stable in C₆D₅Br or C₆D₅Cl, the methyl species immediately underwent solvent activation in CH₂Cl₂ to form the highly fluxional, monomeric chloride cation [Ti(N^tBu)(Me₃[9]aneN₃)Cl]⁺.²² In contrast, [Ti(N^tBu)(Me₃[9]aneN₃)CH₂SiMe₃]⁺ was stable for days in

CH₂Cl₂. To underpin the further studies described below, we briefly investigated the reactivity and properties of alkyl cations derived from some of the other new dialkyls.



We previously studied the different nonclassical interactions in the formally 14-valence-electron cations [Ti(N^tBu)(Me₃[9]aneN₃)R]⁺ (R = Me or CH₂SiMe₃) and the corresponding DFT model systems [Ti(NMe)(H₃[9]aneN₃)R]⁺ (**I-Me** or **I-CH₂SiMe₃**).²² For R = Me only a very weak α-C–H⋯Ti agostic interaction was found, whereas for R = CH₂SiMe₃ a significant β-Si–C⋯Ti agostic interaction was present. Since benzyl ligands are known to stabilize electron-deficient centers through M⋯C_{ipso} interactions,^{53–56} we attempted to observe spectroscopically a monoalkyl cation derived from Ti(N^tBu)(Me₃[9]aneN₃)(CH₂Ph)₂ (**5**). Reaction of **5** with TB in C₆D₅Br yielded the expected organic side-product Ph₃CCH₂Ph and an insoluble orange-brown oil, which could not be further characterized. This is in contrast to the analogous reactions of **1** and **3** forming C₆D₅Br-soluble [Ti(N^tBu)(Me₃[9]aneN₃)R][BAr^F₄]⁺.²² The corresponding reaction of **5** with TB in CD₂Cl₂ quantitatively formed the chloride cation [Ti(N^tBu)(Me₃[9]aneN₃)Cl]⁺.²² This reactivity is analogous to that of **1** but contrasts that of **3** since [Ti(N^tBu)(Me₃[9]aneN₃)CH₂SiMe₃]⁺ was stable in CD₂Cl₂. We previously found that reaction of **1** with neutral BAr^F₃ gave the C₆D₅Br-soluble solvent-separated ion pair [Ti(N^tBu)(Me₃[9]aneN₃)Me][MeBAr^F₃], although reaction of **3** with this reagent gave unidentified mixtures.²² Unfortunately, reaction of **5** with BAr^F₃ in C₆D₅Br again gave an insoluble oil. The soluble portion of the reaction product was a complex mixture of unidentified species.

Although the real benzyl cation [Ti(N^tBu)(Me₃[9]aneN₃)(CH₂Ph)]⁺ could not be observed experimentally, we have used

(50) Fletcher, D. A.; McMeeking, R. F.; Parkin, D. *J. Chem. Inf. Comput. Sci.* **1996**, *36*, 746 (The United Kingdom Chemical Database Service).

(51) Allen, F. H.; Kennard, O. *Chem. Des. Automation News* **1993**, *8*, 1&31.

(52) Kaltsoyannis, N.; Mountford, P. *J. Chem. Soc., Dalton Trans.* **1999**, 781.

(53) Bei, X.; Swenson, D. C.; Jordan, R. F. *Organometallics* **1997**, *16*, 3282.

(54) Wu, F.; Dash, A. K.; Jordan, R. F. *J. Am. Chem. Soc.* **2004**, *126*, 15360.

(55) Chen, Y.-X.; Marks, T. J. *Organometallics* **1997**, *16*, 3649.

(56) Bochmann, M.; Lancaster, S. J. *Organometallics* **1993**, *12*, 633.

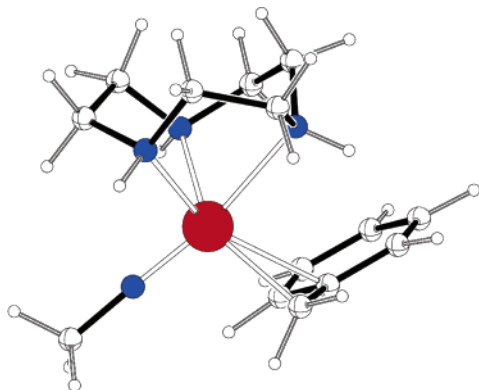


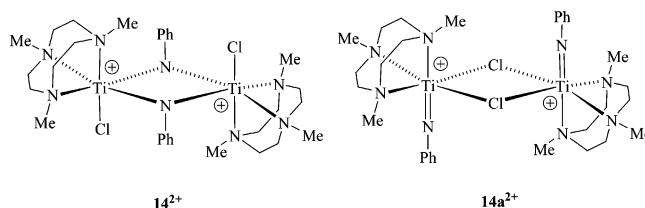
Figure 3. DFT structure of $[\text{Ti}(\text{NMe})(\text{H}_3[9]\text{aneN}_3)\text{CH}_2\text{Ph}]^+$ (**I-CH₂Ph**).

a DFT calculation of the model species $[\text{Ti}(\text{NMe})(\text{H}_3[9]\text{aneN}_3)\text{CH}_2\text{Ph}]^+$ (**I-CH₂Ph**) to gain insights into its structure. The computed geometry of **I-CH₂Ph** is shown in Figure 3 and exhibits a pronounced η^2 -coordination of the benzyl ligand.^{53–56} This is manifested in an acute $\text{Ti}-\text{CH}_2-\text{C}_{\text{ipso}}$ angle of 85.6° and a $\text{Ti}\cdots\text{C}_{\text{ipso}}$ contact of only 2.513 \AA . The geometry of **I-CH₂Ph** is reminiscent of that for **I-CH₂SiMe₃**, where a $\text{Ti}-\text{CH}_2-\text{Si}$ angle of 90.7° and $\text{Ti}\cdots\text{Si}$ and $\text{Ti}\cdots\text{C}_\beta$ distances of 2.841 and 2.534 \AA were calculated. To estimate the strength of the $\text{Ti}\cdots\text{C}_{\text{ipso}}$ interaction in **I-CH₂Ph**, a DFT calculation was carried out on a model species with all the angles subtended at the $\text{Ti}-\text{CH}_2-\text{Ph}$ methylene carbon fixed at 109.5° . This constrained structure was 25.5 kJ mol^{-1} less stable than **I-CH₂Ph**. A similar calculation has been carried out on **I-CH₂SiMe₃**,²² and in this case the constrained geometry was only 14.8 kJ mol^{-1} less stable than the optimized one. Analogous calculations on $[\text{Ti}(\text{NMe})(\text{H}_3[9]\text{aneN}_3)\text{Me}]^+$ (**I-Me**) estimated the $\alpha\text{-C}-\text{H}\cdots\text{Ti}$ agostic interaction as providing less than 2 kJ mol^{-1} stabilization. Therefore, the presence of nonclassical interactions in the imido titanium alkyl cations $[\text{Ti}(\text{N}^t\text{Bu})(\text{Me}_3[9]\text{aneN}_3)\text{R}]^+$ ($\text{R} = \text{CH}_2\text{SiMe}_3, \text{CH}_2\text{Ph}$) can provide significant additional stabilization. Interestingly, although the extra stabilization present in the real system $[\text{Ti}(\text{N}^t\text{Bu})(\text{Me}_3[9]\text{aneN}_3)\text{CH}_2\text{Ph}]^+$ is probably greater than in $[\text{Ti}(\text{N}^t\text{Bu})(\text{Me}_3[9]\text{aneN}_3)\text{CH}_2\text{SiMe}_3]^+$, it is the latter species that has the better stability in CH_2Cl_2 . The tendency for solvent activation ($\text{R} = \text{Me}, \text{CH}_2\text{Ph}$ or CH_2SiMe_3) in the three types of cation $[\text{Ti}(\text{N}^t\text{Bu})(\text{Me}_3[9]\text{aneN}_3)\text{R}]^+$ is therefore not correlated with these nonclassical ground-state stabilization effects, at least according to these gas-phase model systems.

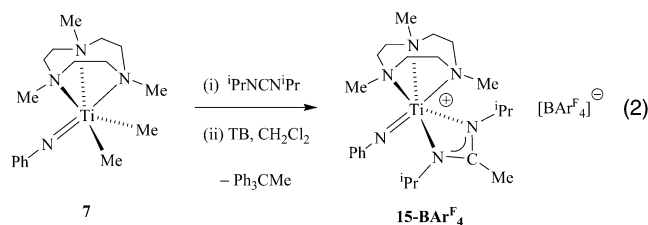
We have built up a good understanding of the properties and reactivity of the *tert*-butyl imido cations $[\text{Ti}(\text{N}^t\text{Bu})(\text{Me}_3[9]\text{aneN}_3)\text{R}]^+$.^{21,22} However, a number of the polymerization experiments described below are based on aryl imido precursors, and it is well established that these can sometimes have different reactivity from that of their alkyl imido analogues.^{17,57} Selected reactivity studies were therefore carried out on the phenyl imide **7** as the parent member of the aryl-substituted series **7–11**.

Addition of TB (1 equiv) to a solution of $\text{Ti}(\text{NPh})(\text{Me}_3[9]\text{aneN}_3)\text{Me}_2$ (**7**) in $\text{C}_6\text{D}_5\text{Br}$ again gave an insoluble oil (cf. the dibenzyl **5**). Other aryl imides studied and also the isopropyl imide **6** showed similar behavior. Reaction of **7** with TB in CD_2Cl_2 formed the expected side-product Ph_3CMe and a mixture of species. After 2 days a single phenyl imido product was present according to the ^1H NMR spectrum. The reaction was successfully scaled up in CH_2Cl_2 , affording the dimeric chloride

derivative $[\text{Ti}_2(\mu\text{-NPh})_2(\text{Me}_3[9]\text{aneN}_3)_2\text{Cl}_2][\text{BAR}^{\text{F}_4}]_2$, **14-BAR^F₄**, in 74% yield. Thus, just as for the *tert*-butyl imido cations $[\text{Ti}(\text{N}^t\text{Bu})(\text{Me}_3[9]\text{aneN}_3)\text{R}]^+$ ($\text{R} = \text{Me}, \text{CH}_2\text{Ph}$), the $\text{Ti}-\text{Me}$ bond of the putative transient methyl cation $[\text{Ti}(\text{NPh})(\text{Me}_3[9]\text{aneN}_3)-\text{Me}]^+$ readily underwent solvent activation.



The ^1H and ^{13}C NMR spectra of **14-BAR^F₄** were sharp at room temperature and consistent with a C_{2v} or C_{2h} -symmetric titanium species. In contrast, those of $[\text{Ti}(\text{N}^t\text{Bu})(\text{Me}_3[9]\text{aneN}_3)\text{Cl}]^+$ and also $[\text{Ti}(\text{N}^t\text{Bu})(\text{Me}_3[9]\text{aneN}_3)\text{R}]^+$ ($\text{R} = \text{Me}$ or CH_2SiMe_3) were very broad and consistent with the complexes being five-coordinate fluxional monomers.²² On the basis of these observations and our experience of these macrocycle-imido systems in general, the sharp spectra for **14-BAR^F₄** indicate that the titanium centers are six-coordinate and that the product contains a dimeric dication. The most likely structure is $[\text{Ti}_2(\mu\text{-NPh})_2(\text{Me}_3[9]\text{aneN}_3)_2\text{Cl}_2]^{2+}$ (**14²⁺**), with bridging phenyl imido ligands, although a chloride-bridged dimer $[\text{Ti}_2(\text{NPh})_2(\text{Me}_3[9]\text{aneN}_3)_2(\mu\text{-Cl})_2]^{2+}$ (**14a²⁺**) is in principle also feasible. Isomer **14²⁺** is favored over **14a²⁺** since Teuben et al. have reported dimeric imido-bridged species $\text{Cp}_2\text{Ti}_2(\mu\text{-NR})_2\text{Cl}_2$ ($\text{R} = \text{Et}, ^i\text{Pr}, ^t\text{Bu}, \text{Ph}$), which are the isolobal analogues of **14²⁺/14a²⁺**.⁵⁸ The homologue $\text{Cp}^*\text{Ti}_2(\mu\text{-NTol})_2\text{Cl}_2$ is also dimeric.⁵⁹ The differing behavior of five-coordinate $[\text{Ti}(\text{N}^t\text{Bu})(\text{Me}_3[9]\text{aneN}_3)\text{Cl}]^+$ versus dimeric **14²⁺** reflects the reduced steric protection at the imido nitrogen atoms in the latter. A related pair of complexes from the recent imido titanium literature are the crystallographically characterized $\text{Ti}(\eta\text{-C}_8\text{H}_8)(\text{N}^t\text{Bu})$ and $\text{Ti}_2(\eta\text{-C}_8\text{H}_8)_2(\mu\text{-NPh})_2$.⁶⁰ Unfortunately, we were not able to obtain diffraction-quality crystals of **14-BAR^F₄** or to obtain a useful mass spectrum to support our conclusions.



Further experiments were carried out to gain evidence for the transient methyl cation $[\text{Ti}(\text{NPh})(\text{Me}_3[9]\text{aneN}_3)\text{Me}]^+$. We recently reported that $[\text{Ti}(\text{N}^t\text{Bu})(\text{Me}_3[9]\text{aneN}_3)\text{CH}_2\text{SiMe}_3]^+$ reacts with diisopropylcarbodiimide to form the insertion product $[\text{Ti}(\text{N}^t\text{Bu})(\text{Me}_3[9]\text{aneN}_3)\{\text{Me}_3\text{SiCH}_2\text{C}(\text{N}^i\text{Pr})_2\}]^+$. Furthermore, generating the methyl cation $[\text{Ti}(\text{N}^t\text{Bu})(\text{Me}_3[9]\text{aneN}_3)\text{Me}]^+$ in CH_2Cl_2 in the presence of TMA quantitatively yielded the adduct $[\text{Ti}(\text{N}^t\text{Bu})(\text{Me}_3[9]\text{aneN}_3)(\mu\text{-Me})_2\text{AlMe}_2]^+$.²¹

As shown in eq 2, reaction of $\text{Ti}(\text{NPh})(\text{Me}_3[9]\text{aneN}_3)\text{Me}_2$ (**7**) with TB in CH_2Cl_2 in the presence of diisopropylcarbodiimide successfully gave the acetamidinate derivative $[\text{Ti}(\text{NPh})(\text{Me}_3[9]\text{aneN}_3)\{\text{MeC}(\text{N}^i\text{Pr})_2\}][\text{BAR}^{\text{F}_4}]$ (**15-BAR^F₄**) as a yellow powder in 44% isolated yield. When the reaction was carried out on

(58) Vroegop, C. T.; Teuben, J. H.; van Bolhuis, F.; van der Linden, J. G. M. *J. Chem. Soc., Chem. Commun.* **1983**, 550.

(59) Guiducci, A. E. D.Phil. Thesis, University of Oxford, 2002.

(60) Dunn, S. C.; Hazari, N.; Jones, N. M.; Moody, A. G.; Blake, A. J.; Cowley, A. R.; Green, J. C.; Mountford, P. *Chem. Eur. J.* **2005**, *11*, 2111.

(57) Gade, L. H.; Mountford, P. *Coord. Chem. Rev.* **2001**, *216–217*, 65.

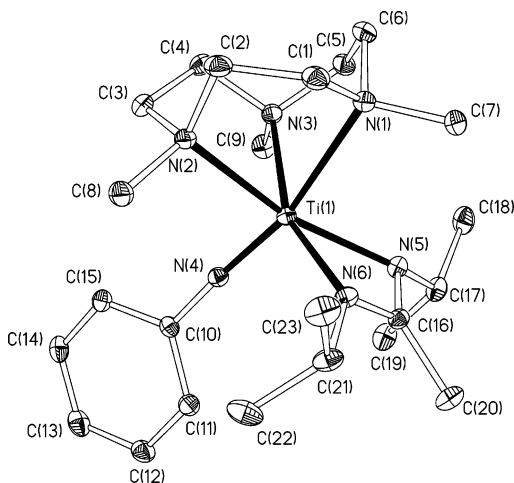


Figure 4. Displacement ellipsoid plot (20% probability) of the cation $[\text{Ti}(\text{NPh})(\text{Me}_3[9]\text{aneN}_3)\{\text{MeC}(\text{N}^i\text{Pr})_2\}]^+$ ($\mathbf{15}^+$). H atoms are omitted.

Table 2. Selected Bond Lengths (Å) and Angles (deg) for $[\text{Ti}(\text{NPh})(\text{Me}_3[9]\text{aneN}_3)\{\text{MeC}(\text{N}^i\text{Pr})_2\}]^+$ ($\mathbf{15}^+$)

Ti(1)–N(1)	2.4157(16)	Ti(1)–N(6)	2.1010(15)
Ti(1)–N(2)	2.2750(16)	N(4)–C(10)	1.386(2)
Ti(1)–N(3)	2.2515(15)	C(16)–N(5)	1.339(2)
Ti(1)–N(4)	1.7248(16)	C(16)–N(6)	1.342(2)
Ti(1)–N(5)	2.1275(15)	C(16)–N(6)	1.508(3)
N(1)–Ti(1)–N(2)	75.47(6)	N(4)–Ti(1)–N(5)	102.36(7)
N(1)–Ti(1)–N(3)	74.93(6)	N(1)–Ti(1)–N(6)	86.26(6)
N(2)–Ti(1)–N(3)	78.17(6)	N(2)–Ti(1)–N(6)	108.26(6)
N(1)–Ti(1)–N(4)	167.26(7)	N(3)–Ti(1)–N(6)	158.09(6)
N(2)–Ti(1)–N(4)	93.77(7)	N(4)–Ti(1)–N(6)	103.85(7)
N(3)–Ti(1)–N(4)	96.44(7)	N(5)–Ti(1)–N(6)	64.24(6)
N(1)–Ti(1)–N(5)	88.94(6)	Ti(1)–N(4)–C(10)	176.67(14)
N(2)–Ti(1)–N(5)	163.39(6)	N(5)–C(16)–N(6)	114.05(16)
N(3)–Ti(1)–N(5)	103.60(6)		

the NMR tube scale in CD_2Cl_2 , $\mathbf{15}\text{-Bar}^{\text{F}_4}$ was formed in quantitative yield, with no evidence for a competing [2+2] cycloaddition reaction at the $\text{Ti}=\text{NPh}$ bond. The X-ray structure of the cation $\mathbf{15}^+$ is shown in Figure 4, and selected bond lengths and angles are given in Table 2. Consistent with this, the ^1H and ^{13}C NMR spectra for $\mathbf{15}^+$ were indicative of C_s molecular symmetry, and the high-resolution electrospray mass spectrum of $\mathbf{15}\text{-Bar}^{\text{F}_4}$ in MeCN (positive ion mode) showed the expected pattern for the molecular ion $\mathbf{15}^+$. Attempts were also made to generate a bimetallic TMA adduct $[\text{Ti}(\text{NPh})(\text{Me}_3[9]\text{aneN}_3)(\mu\text{-Me}_2\text{AlMe}_2)]^+$, but only complex mixtures were formed.

Cation $\mathbf{15}^+$ contains an approximately octahedral titanium center with a *fac*-coordinated macrocycle, a terminal phenyl imido group, and a diisopropylacetamidate ligand. All of the $\text{Ti}-\text{N}_{\text{macrocycle}}$ distances and the $\text{Ti}-\text{N}_{\text{imido}}$ distance are slightly shorter than in the dimethyl precursor $\text{Ti}(\text{NPh})(\text{Me}_3[9]\text{aneN}_3)\text{-Me}_2$ (**7**), which can be attributed to the cationic nature of $\mathbf{15}^+$. The *trans* influence of the imido ligand is apparent from the elongation of the $\text{Ti}(1)-\text{N}(1)$ bond relative to $\text{Ti}(1)-\text{N}(2)$ and $\text{Ti}(1)-\text{N}(3)$. The bond lengths within the acetamidate ligand are the same within error as those in the analogue $[\text{Ti}(\text{N}^i\text{Bu})(\text{Me}_3[9]\text{aneN}_3)\{\text{Me}_3\text{SiCH}_2\text{C}(\text{N}^i\text{Pr})_2\}]^+$.²¹ The formation of $\mathbf{15}^+$ shows clearly that a monomethyl cation was successfully generated from **7**.

Ethylene Polymerization Studies. A principal aim of this work was to determine the structure–productivity relationships for ethylene polymerization by a homologous series of well-defined imido titanium dialkyl precatalysts in the absence of MAO. Although bis(trimethylsilylmethyl) derivatives $\text{Ti}(\text{NR})(\text{Me}_3[9]\text{aneN}_3)(\text{CH}_2\text{SiMe}_3)_2$ have been prepared for $\text{R} = ^i\text{Bu}$

(**3**), ^iPr (**12**), and Ar^{F} (**13**, very low yield), it was not possible to obtain other members of this family. Therefore we focused on the series of dimethyl compounds $\text{Ti}(\text{NR})(\text{Me}_3[9]\text{aneN}_3)\text{Me}_2$ ($\text{R} = ^i\text{Bu}$ (**1**), ^iPr (**6**), Ph (**7**), 3,5- $\text{C}_6\text{H}_3(\text{CF}_3)_2$ (**8**), 2,6- $\text{C}_6\text{H}_3^i\text{Pr}_2$ (**9**), 2- $\text{C}_6\text{H}_4\text{CF}_3$ (**10**), 2- $\text{C}_6\text{H}_4^i\text{Bu}$ (**11**)). In addition to these precatalysts, the other *tert*-butyl imides $\text{Ti}(\text{N}^i\text{Bu})(\text{Me}_3[9]\text{aneN}_3)\text{R}_2$ ($\text{R} = \text{CH}_2\text{SiMe}_3$ (**3**) and CH_2Ph (**5**)) were also studied to probe for potential initiator effects⁶¹ arising from the different precatalyst alkyl groups.

TB was chosen as a methide ion abstraction reagent, as this has proved successful in a range of previous systems^{4,30,32} and in the stoichiometric cation chemistry derived from $\text{Ti}(\text{NR})(\text{Me}_3[9]\text{aneN}_3)\text{R}'_2$ as described above and elsewhere.^{20–23} Ethylene polymerization experiments are typically conducted in the presence of a scavenger to reduce the background level of trace impurities (typically H_2O) in the system since the highly electrophilic and electron-deficient alkyl cations are very reactive. TIBA is routinely used as a scavenger in dialkyl catalyst systems using borane or borate activators.^{30,32} It is generally thought that the bulky nature of the isobutyl groups disfavors the formation of adducts of the kind $[\text{L}_n\text{M}(\mu\text{-R})_2\text{AlR}_2]^+$, making these systems more highly active than the related MAO-activated systems (typically containing 20–30% TMA, which coordinates well to alkyl cations^{35–44}). However, it is also recognized that the chemistry of TIBA-based activator systems is complex, and we address the reactions of neutral and cationic imido titanium alkyl compounds with TIBA later in this paper.^{30,32,62–65}

Polymerization experiments were performed in toluene under 6 bar ethylene pressure with room-temperature initiation in order to make as close a comparison as possible with the recently reported results for the $\text{Ti}(\text{NR})(\text{Me}_3[9]\text{aneN}_3)\text{Cl}_2/\text{MAO}$ catalyst systems where available ($\text{R} = ^i\text{Bu}$, Ph, 2,6- $\text{C}_6\text{H}_3^i\text{Pr}_2$, 2- $\text{C}_6\text{H}_4\text{-CF}_3$, 2- $\text{C}_6\text{H}_4^i\text{Bu}$).²³ Catalysis runs were typically carried out in duplicate and were generally reproducible with $\pm 10\%$ of the mean values reported. Full details are given in the Experimental Section.

Productivities. Table 3 summarizes the results of the polymerization experiments. We consider first the dimethyl systems (entries 1–10). The *tert*-butyl imide **1** provides the most productive system of all ($6230 \text{ kg mol}^{-1} \text{ h}^{-1} \text{ bar}^{-1}$), and among the aryl imides the bulkiest precatalyst **11** is the most productive ($1210 \text{ kg mol}^{-1} \text{ h}^{-1} \text{ bar}^{-1}$). The other systems showing non-negligible productivity are **9** and **10** (200 and $105 \text{ kg mol}^{-1} \text{ h}^{-1} \text{ bar}^{-1}$, respectively). Precatalysts **6–8** were effectively inactive. There is therefore a strong correlation between the steric bulk of the imido substituents and catalyst productivity, and we discuss this in further detail below.

The catalyst system **1**/TB/TIBA gave a 75°C temperature rise over the 20 min polymerization run time and produced 24.9 g of PE. The productivity is therefore probably mass transport limited, and the changing reaction conditions may impact on the PE molecular weights and their distribution.³² However, attempts to reduce the catalyst loading below $2 \mu\text{mol}$ of **1** in 250 mL of toluene gave substantial decreases in productivity. For example, at $1 \mu\text{mol}$ loading of **1** (with the same quantity of TIBA as in entry 1) the PE yield was 1.81 g ($905 \text{ kg mol}^{-1} \text{ h}^{-1} \text{ bar}^{-1}$). Therefore the excellent productivity listed for **1** should

(61) Mehrkhodavandi, P.; Schrock, R. R.; Pryor, L. L. *Organometallics* **2003**, *22*, 4569.

(62) Song, F.; Cannon, R. D.; Lancaster, S. J.; Bochmann, M. *J. Mol. Catal. A: Chem.* **2004**, *218*, 21.

(63) Götz, C.; Rau, A.; Luft, G. *J. Mol. Catal. A: Chem.* **2002**, *184*, 95.

(64) Bochmann, M.; Sarsfield, M. J. *Organometallics* **1998**, *17*, 5908.

(65) Carr, A. G.; Dawson, D. M.; Thornton-Pett, M.; Bochmann, M. *Organometallics* **1999**, *18*, 2933.

Table 3. Ethylene Polymerization Data for Ti(NⁱBu)(Me₃[9]aneN₃)R₂ (R = Me (1), CH₂SiMe₃ (3), CH₂Ph (5)) and Ti(NR)(Me₃[9]aneN₃)Me₂ (R = ⁱPr (6), Ph (7), 3,5-C₆H₃(CF₃)₂ (8), 2,6-C₆H₃ⁱPr₂ (9), 2-C₆H₄CF₃ (10), and 2-C₆H₄ⁱBu (11))^a

entry	precatalyst	additional comment	yield of PE (g)	productivity (kg mol ⁻¹ h ⁻¹ bar ⁻¹)	M _w (g mol ⁻¹)	M _n (g mol ⁻¹)	M _w /M _n
1	Ti(N ⁱ Bu)(Me ₃ [9]aneN ₃)Me ₂ (1)		24.9	6230	19 700	7130	2.8
2	Ti(N ⁱ Pr)(Me ₃ [9]aneN ₃)Me ₂ (6)		0.04	10	<i>b</i>	<i>b</i>	<i>b</i>
3	Ti(NPh)(Me ₃ [9]aneN ₃)Me ₂ (7)		0	0			
4	Ti(N-3,5-C ₆ H ₃ (CF ₃) ₂)(Me ₃ [9]aneN ₃)Me ₂ (8)		0.02	5	<i>b</i>	<i>b</i>	<i>b</i>
5	Ti(N-2,6-C ₆ H ₃ Pr ₂)(Me ₃ [9]aneN ₃)Me ₂ (9)		0.80	200	342 000	54 600	6.3
6	Ti(N-2-C ₆ H ₄ CF ₃)(Me ₃ [9]aneN ₃)Me ₂ (10)		0.41	105	380 000	137 000	2.8
7	Ti(N-2-C ₆ H ₄ ⁱ Bu)(Me ₃ [9]aneN ₃)Me ₂ (11)		4.8	1210	474 000	158 000	3.0
8	Ti(N-2-C ₆ H ₄ ⁱ Bu)(Me ₃ [9]aneN ₃)Me ₂ (11)	<i>c</i>	8.7	2180	245 000	92 400	2.7
9	Ti(NPh)(Me ₃ [9]aneN ₃)Me ₂ (7)	<i>c</i>	0	0			
10	Ti(N-2-C ₆ H ₄ CF ₃)(Me ₃ [9]aneN ₃)Me ₂ (10)	<i>c</i>	0.43	110	244 000	82 800	3.0
11	Ti(N ⁱ Bu)(Me ₃ [9]aneN ₃)(CH ₂ SiMe ₃) ₂ (3)		0.53	130	118 600	39 500	3.0
12	Ti(N ⁱ Bu)(Me ₃ [9]aneN ₃)(CH ₂ Ph) ₂ (5)		0.48	120	83 800	29 100	2.9
13	Ti(N ⁱ Bu)(Me ₃ [9]aneN ₃)(CH ₂ SiMe ₃) ₂ (3)	<i>c</i>	0.29	75	<i>b</i>	<i>b</i>	<i>b</i>
14	Ti(N ⁱ Bu)(Me ₃ [9]aneN ₃)(CH ₂ Ph) ₂ (5)	<i>c</i>	0.45	115	<i>b</i>	<i>b</i>	<i>b</i>
15	Ti(N ⁱ Bu)(Me ₃ [9]aneN ₃)Me ₂ (1)	<i>d</i>	0.90	225	134 500 ^e	30 400 ^e	4.4

^a Conditions unless stated otherwise: 6 bar of C₂H₄ on demand, 2 μmol of precatalyst, 1 equiv of TB, 5 mmol of TIBA, 250 mL of toluene, 1 L reactor, 20 min, initiated at 22–24 °C. ^bNot recorded. ^cInitiated at 35 °C. ^dNo added TB. ^eBimodal polymer with M_p = 51 100 and 165 500 g mol⁻¹. See Experimental Section for other details.

in fact be viewed as a lower limit, and the polydispersity index (PDI, M_w/M_n) as the least favorable. These limitations for **1** do not detract from our overall ability to establish qualitative structure–productivity correlations within the family of imides evaluated.

The catalyst system **11**/TB/TIBA appeared to show an induction period. Monitoring of the ethylene uptake rate (flow rate into the reactor) showed a significant increase after ca. 10 min, which was accompanied by a ca. 10 °C rise in temperature. This polymerization experiment was repeated with an initiation temperature of 35 °C (entry 8, Table 3), which gave an increase in polymer yield from 4.8 g (1210 kg mol⁻¹ h⁻¹ bar⁻¹) to 8.7 g (2180 kg mol⁻¹ h⁻¹ bar⁻¹) and an ethylene uptake at the higher flow rate from the beginning of the experiment. For comparison, the catalyst systems **7**/TB/TIBA and **10**/TB/TIBA were also evaluated at the 35 °C initiation temperature (entries 9 and 10). In these cases no productivity gain was observed.

Somewhat surprisingly, the productivities for the other *tert*-butyl imides Ti(NⁱBu)(Me₃[9]aneN₃)R₂ (R = CH₂SiMe₃ (**3**), CH₂Ph (**5**)) were very disappointing, both at 22–24 °C initiation (130 and 120 kg mol⁻¹ h⁻¹ bar⁻¹, entries 11 and 12) and at 35 °C (75 and 115 kg mol⁻¹ h⁻¹ bar⁻¹, entries 13 and 14). Likely origins of this behavior will be discussed later. We also evaluated the ethylene polymerization capability of **1**/TIBA in the absence of TB activator (entry 15, Table 3).⁶⁶ This run resulted in 0.90 g of PE in 20 min, corresponding to a productivity of 225 kg mol⁻¹ h⁻¹ bar⁻¹, demonstrating that the reaction between **1** and TIBA produces a reasonably active catalyst, but that this productivity is negligible compared to that with TB present. TIBA alone has also been used as an activator in other catalyst systems.^{67,68}

Polymer Properties. The PEs produced by the more active catalyst systems were analyzed by GPC (Table 3). The M_w values are typically in the range 10⁵–10⁶ g mol⁻¹. With the exception of the PEs from **9**/TB/TIBA and **1**/TIBA, the polymers were unimodal with PDIs between 2.7 and 3.0. Although the Schultz–Flory distribution⁶⁹ predicts that a single-site catalyst undergoing chain transfer processes should give rise to a

polymer having a PDI of 2.0, the values of 2.7–3.0 are still consistent with single-site type catalysts. PDIs greater than 2.0 can be attributed to the presence of more than one active species, or polymerization conditions changing over time, due for example to a large exotherm or polymer precipitation during the experiment. For the **9**/TB/TIBA catalyst system the GPC analysis showed a single broad fraction, whereas for **1**/TIBA the sample was clearly bimodal with M_p values of 51 100 and 165 500 (overall M_w = 134 500, PDI = 4.4).

The molecular weight of the PE formed with **1**/TB/TIBA was much lower than those of the other samples. This is attributed to the larger exotherm during the polymerization process since chain transfer has a higher activation energy than propagation.⁷⁰ The same effect can be seen when comparing the PEs formed with **10** and **11** at ambient temperature (entries 6 and 7 in Table 3) and 35 °C (entries 8 and 10).

The M_n values for the PE produced with **1**/TB/TIBA suggest that ca. 1750 PE chains are formed per metal center, assuming that all are productive. In contrast, with the exception of **11**/TB/TIBA at 35 °C initiating temperature (ca. 50 chains per metal), the other catalyst systems produce only ca. 10–15 chains per titanium present. This may indicate that fewer precatalyst centers are actually activated/active and/or that efficient chain transfer is more energetically accessible at higher temperatures.⁷⁰ It has been suggested that chain transfer to TIBA is disfavored in zirconocene systems due to unfavorable steric interactions in forming the necessary isobutyl-bridged heteronuclear bimetallic intermediate.^{71,72} Diiminopyridyl iron catalysts, on the other hand, have been shown to readily undergo chain transfer with TIBA and also the Al-ⁱBu groups of MMAO, giving isopropyl-terminated polymer chains.⁷³

We also note Brintzinger's proposal that, at elevated temperatures, aluminum hydride species may be formed from TIBA by loss of isobutene and that chain transfer to these hydride species would be more favored relative to chain transfer to TIBA itself.⁷² However, the ¹H NMR spectrum of our TIBA in C₆D₆ showed no evidence for aluminum hydrides present in greater

(66) The TB/TIBA mixture alone does not act as a catalyst system under the conditions used in this study.

(67) Franceschini, F. C.; Tavares, T. T. d. R.; Greco, P. P.; Galland, G. B.; dos Santos, J. H. Z.; Soares, J. B. P. *J. Appl. Polym. Sci.* **2005**, *95*, 1050.

(68) Bryliakov, K. P.; Semikolenova, N. V.; Zakharov, V. A.; Talsi, E. P. *Organometallics* **2004**, *23*, 5375.

(69) Flory, P. J. *Principles of Polymer Chemistry*; Cornell University Press: Ithaca, NY, 1992.

(70) D'Agillo, L.; Soares, J. B. P.; Penlidis, A. *Macromol. Chem. Phys.* **1998**, *199*, 955.

(71) Lieber, S.; Brintzinger, H. H. *Macromolecules* **2000**, *33*, 9192.

(72) Bhriain, N. N.; Brintzinger, H. H.; Ruchatz, D.; Fink, G. *Macromolecules* **2005**, *38*, 2056.

(73) Small, B. L.; Brookhart, M. *Macromolecules* **1999**, *32*, 2120.

than 1% quantities. Furthermore, heating this solution in a sealed NMR tube at 80 °C for 20 min (the run-times used in the polymerization experiments) gave no change in the appearance of the spectrum or decay of the TIBA resonances as judged by integration against an internal toluene standard. Nonetheless, it may still be possible that aluminum-hydride species play a role under the experimental polymerization conditions.

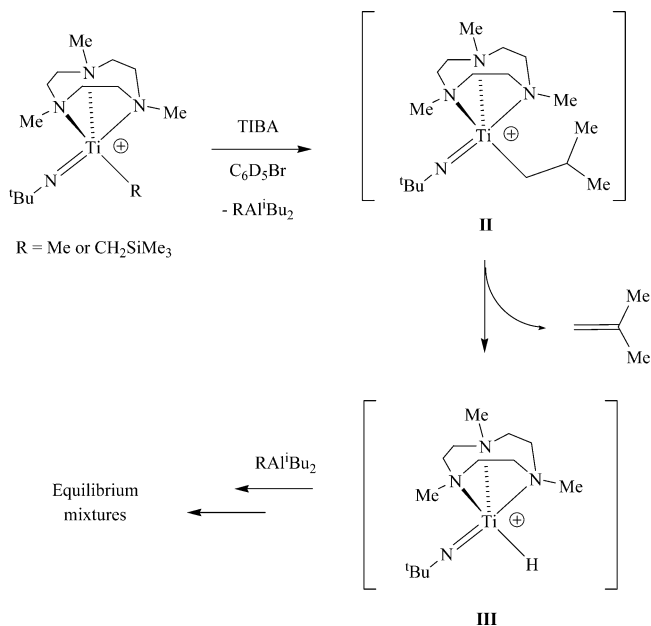
Experiments on the Ti(N^tBu)(Me₃[9]aneN₃)Cl₂/MAO catalyst system identified two chain transfer mechanisms,²³ namely, chain transfer to TMA, which results in methyl end groups, and β-H transfer (either to metal or direct to monomer), resulting in vinyl-terminated PE. A series of experiments in which the amount of free TMA was varied showed that as the TMA:Ti ratio increased, the amount of chain transfer to TMA also increased, resulting in fewer vinyl-terminated PE chains and lower molecular weights.

The PE sample from the 1/TB/TIBA catalyst system was analyzed by NMR spectroscopy in 1,2-C₆D₄Cl₂ at 100 °C. The PE contained no detectable vinyl end groups, therefore indicating that chain termination by β-H transfer is not significant in this system. However, no isopropyl end groups were observed either, which at first sight would have been the expectation for a mechanism involving chain transfer to TIBA followed by renewed chain growth at a Ti-CH₂ⁱPr group.⁷³ This aspect is discussed further below. By assuming two methyl end groups per chain, analysis of the PE ¹H integrals gave *M_n* = 7300 g mol⁻¹, a value very close to the *M_n* = 7130 g mol⁻¹ determined by GPC. We also attempted to analyze the PE from the 11/TB/TIBA (35 °C initiation) catalyst system by ¹H NMR. Unfortunately the PE was too insoluble for any end group analysis to be carried out.

Comparison with the Ti(NR)(Me₃[9]aneN₃)Cl₂/MAO Catalyst Systems. It is interesting to compare the reported ethylene polymerization capability of the dichloride precatalysts Ti(NR)(Me₃[9]aneN₃)Cl₂ (R = ^tBu, Ph, 2,6-C₆H₃ⁱPr₂, 2-C₆H₄CF₃, 2-C₆H₄^tBu). These were activated with MAO (Al:Ti ratio = 1500:1) at ambient temperature under conditions otherwise comparable to those used here.²³ The aryl imido systems showed structure–productivity and PDI trends broadly comparable to those for the TB/TIBA-activated dimethyl systems: for R = Ph, productivity < 1 kg mol⁻¹ h⁻¹ bar⁻¹; for R = 2,6-C₆H₃ⁱPr₂, productivity = 120 kg mol⁻¹ h⁻¹ bar⁻¹ (PDI = 7.9); for R = 2-C₆H₄CF₃, productivity = 220 kg mol⁻¹ h⁻¹ bar⁻¹ (PDI = 2.4); for R = 2-C₆H₄^tBu, productivity = 580 kg mol⁻¹ h⁻¹ bar⁻¹ (PDI = 3.3). Interestingly, whereas Ti(N^tBu)(Me₃[9]aneN₃)-Me₂ (**1**) is 5 times as productive as Ti(N-2-C₆H₄^tBu)(Me₃[9]aneN₃)Me₂ (**11**) in the dimethyl/TB/TIBA systems, it was found that Ti(N^tBu)(Me₃[9]aneN₃)Cl₂/MAO had a comparable activity (630 kg mol⁻¹ h⁻¹ bar, PDI = 4.3) to that of Ti(N-2-C₆H₄^tBu)(Me₃[9]aneN₃)Cl₂/MAO. Nonetheless, despite these differences between the two catalyst systems, it is clear that both the dimethyl/TB/TIBA and dichloride/MAO catalyst families require a bulky imido substituent to achieve high productivities.

Reactions of [Ti(NR)(Me₃[9]aneN₃)R']⁺ and Ti(NR)(Me₃[9]aneN₃)R'₂ with TIBA: NMR and DFT Studies. A focused series of NMR tube scale experiments and selected DFT calculations was carried out. While the chemistry of the imido titanium alkyl systems with TIBA is likely to be very complex,^{30,32,71,72} it was hoped that additional insights could be gained regarding certain aspects of this work, namely, the dependence of productivity on steric bulk at the imido nitrogen, the formation of saturated PE chains in the 1/TB/TIBA catalyst system, and the apparent chain transfer to aluminum within the systems studied.

Scheme 2. Reaction of [Ti(N^tBu)(Me₃[9]aneN₃)R]⁺ with TIBA in C₆D₅Br at -30 °C (R = Me or CH₂SiMe₃)



Reaction of [Ti(N^tBu)(Me₃[9]aneN₃)R]⁺ (R = Me or CH₂SiMe₃) with TIBA. We previously showed that reaction of the methyl cation [Ti(N^tBu)(Me₃[9]aneN₃)Me]⁺ with TMA in C₆D₅Br cleanly and quantitatively formed [Ti(N^tBu)(Me₃[9]aneN₃)(μ-Me)₂AlMe₂]⁺.²¹ Analogous reactions were therefore performed between [Ti(N^tBu)(Me₃[9]aneN₃)R]⁺ (R = Me or CH₂SiMe₃) and TIBA. As mentioned above, attempts to generate other imido titanium alkyl cations in C₆D₅Br gave oily precipitates, and so the corresponding reactions with TIBA were not carried out for these. Addition of TIBA (1 equiv) to preformed [Ti(N^tBu)(Me₃[9]aneN₃)Me]⁺ in C₆D₅Br at -30 °C immediately formed a mixture of macrocycle- and isobutyl-containing species and isobutene. None of the original reactants remained. No further change took place after 20 min, and the sample was allowed to warm up. After 30 min at room temperature the ¹H NMR spectrum showed two major macrocycle-containing species in a ca. 2:1 ratio by integration. The same mixture was formed when the reaction was repeated entirely at room temperature. In an analogous reaction, [Ti(N^tBu)(Me₃[9]aneN₃)CH₂SiMe₃]⁺ was generated in situ in C₆D₅Br, cooled to -30 °C, and TIBA was added. Again isobutene was formed immediately, along with complete conversion to a mixture of new organometallic species. On warming to room temperature, further changes took place, and ultimately the major macrocycle-containing product was the same as the dominant species formed in the reaction with [Ti(N^tBu)(Me₃[9]aneN₃)Me]⁺. This species appears to possess molecular C_s symmetry and two aluminum-bound isobutyl groups. The ¹⁹F NMR spectrum of the mixtures showed only the expected resonances for [BAR^F₄]⁻, ruling out anion activation, although solvent activation pathways cannot be discounted.⁷⁴

As shown in Scheme 2, the appearance of isobutene in these reactions suggests that the first step (rapid even at -30 °C) is exchange of the Ti-bound alkyl group with one of the isobutyl groups of TIBA to form **II** (Scheme 2), which is followed by rapid β-H elimination. The presence of a mixture of species at -30 °C suggests that this putative first-formed hydride cation⁷⁴

(74) Ma, K.; Piers, W. E.; Gao, Y.; Parvez, M. *J. Am. Chem. Soc.* **2004**, *126*, 5668.

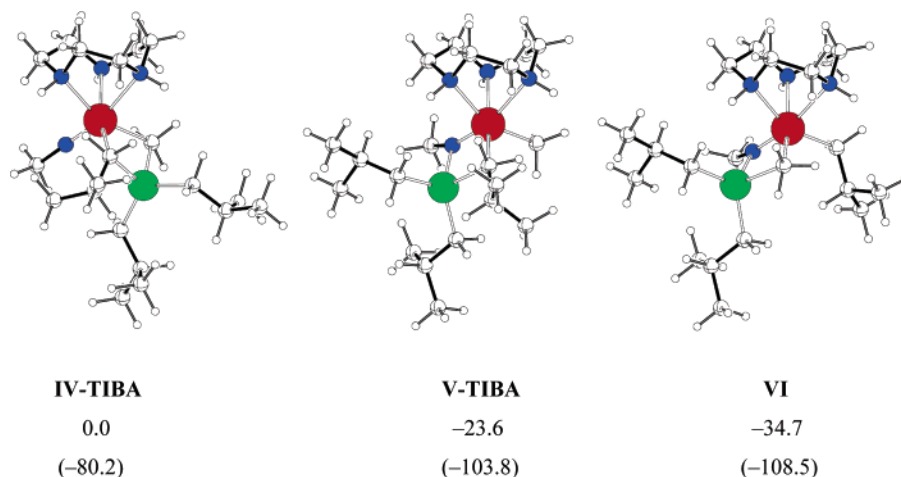


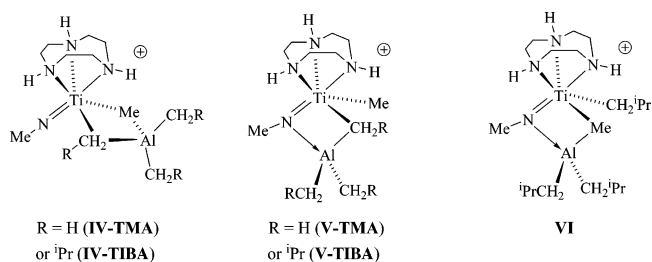
Figure 5. DFT structures of three isomers of the adduct formed between $[\text{Ti}(\text{NMe})(\text{H}_3[9]\text{aneN}_3)\text{Me}]^+$ and TIBA. Relative energies are given in kJ mol^{-1} . The values in parentheses are formation energies with respect to separated $[\text{Ti}(\text{NMe})(\text{H}_3[9]\text{aneN}_3)\text{Me}]^+$ and TIBA (for **IV-TIBA** and **V-TIBA**) or $[\text{Ti}(\text{NMe})(\text{H}_3[9]\text{aneN}_3)^+\text{Bu}]^+$ and MeAl^iBu_2 (for **VI**). Ti, Al, and N atoms are shown in red, green, and blue, respectively.

III and the new alkyl aluminum species RAl^iBu_2 give rise to further reactions. The precise identity of the final dominant product(s) formed on warming to room temperature is unknown, and it was not possible to isolate a pure compound on the preparative scale.

The rapid reaction of $[\text{Ti}(\text{N}^i\text{Bu})(\text{Me}_3[9]\text{aneN}_3)\text{R}]^+$ with TIBA for both $\text{R} = \text{Me}$ or CH_2SiMe_3 supports the view that chain transfer to TIBA could in principle be facile in these catalyst systems. To account for the absence of isopropyl end groups in the PE formed by **1**/TB/TIBA, renewed chain growth following formation of $[\text{Ti}(\text{N}^i\text{Bu})(\text{Me}_3[9]\text{aneN}_3)\text{CH}_2^i\text{Pr}]^+$ (**II**) presumably occurs either after β -H elimination to form **III** (which may then insert C_2H_4 , forming an ethyl cation $[\text{Ti}(\text{N}^i\text{Bu})(\text{Me}_3[9]\text{aneN}_3)\text{-Et}]^+$) or after β -H transfer to monomer, directly forming an ethyl cation and isobutene.³² In other words, the isobutyl cation **II** is not a competitive chain growth initiating species in these catalyst systems.

DFT-Computed TIBA Adducts of $[\text{Ti}(\text{NMe})(\text{H}_3[9]\text{aneN}_3)\text{-Me}]^+$. In the catalyst system $\text{Ti}(\text{N}^i\text{Bu})(\text{Me}_3[9]\text{aneN}_3)\text{Cl}_2/\text{MAO}$, it was found that increasing the amount of TMA present resulted not only in a decrease in M_w and the number of PE vinyl end groups (see above) but also in a decrease of productivity.^{20,23} This was attributed to a higher fraction of the titanium present being trapped as nonproductive resting-state adducts^{35–44} of the type $[\text{Ti}(\text{N}^i\text{Bu})(\text{Me}_3[9]\text{aneN}_3)(\mu\text{-Me})(\mu\text{-R})\text{AlMe}_2]^+$ ($\text{R} = \text{polymeryl}$ or Me^2). The poor productivities of precatalysts $\text{Ti}(\text{NR})(\text{Me}_3[9]\text{aneN}_3)\text{Cl}_2$ with smaller imido R-groups were attributed to a lack of steric protection of the $\text{Ti}=\text{NR}$ linkage toward attack by TMA or other species present. Very recently, we performed DFT calculations on the energies of the potential adducts formed between TMA and the model species $[\text{Ti}(\text{NMe})(\text{H}_3[9]\text{aneN}_3)\text{Me}]^+$ (**IV-TMA**, **V-TMA**; see below).⁷⁵ It is expected that TIBA would be less likely than TMA to form such adducts because of the associated adverse steric effects.^{30,72,76} Nonetheless, the polymerization results and NMR tube scale experiments for $[\text{Ti}(\text{N}^i\text{Bu})(\text{Me}_3[9]\text{aneN}_3)\text{R}]^+$ with TIBA suggest that such interactions are possible in these cases. To better quantify the situation, and to evaluate the types of adducts that might be formed in the $\text{Ti}(\text{NR})(\text{Me}_3[9]\text{aneN}_3)\text{Me}_2/\text{TB}/\text{TIBA}$

catalyst systems, we carried out DFT calculations on three potential products (**IV-TIBA**, **V-TIBA**, and **VI**) formed between the model methyl cation $[\text{Ti}(\text{NMe})(\text{H}_3[9]\text{aneN}_3)\text{Me}]^+$ and TIBA. Line drawing representations are shown below, and the DFT structures themselves are presented in Figure 5.



The bis(μ -alkyl) adduct $[\text{Ti}(\text{NMe})(\text{H}_3[9]\text{aneN}_3)(\mu\text{-Me})(\mu\text{-}^i\text{Bu})\text{-Al}^i\text{Bu}_2]^+$ (**IV-TIBA**) was calculated to have a formation energy of $-80.2 \text{ kJ mol}^{-1}$ relative to separated $[\text{Ti}(\text{NMe})(\text{H}_3[9]\text{aneN}_3)\text{-Me}]^+$ and TIBA. The corresponding model with TMA (**IV-TMA**) had a formation energy of $-98.4 \text{ kJ mol}^{-1}$.⁷⁵ The lower stability of **IV-TIBA** relative to **IV-TMA** is attributable to the bulky isobutyl groups. These results are supported by recent experimental studies by Anwander on neutral ytrocene tetraalkylaluminates $\text{rac}\{-\text{Me}_2\text{Si}(2\text{-C}_9\text{H}_5\text{Me})_2\}\text{Y}(\mu\text{-R})(\mu\text{-R}')\text{AlR}'_2$ ($\text{R} = \text{Me, Et}$; $\text{R}' = \text{Me, Et, }^i\text{Bu}$).⁷⁶ The presence of imido nitrogen lone pairs in the cations $[\text{Ti}(\text{NR})(\text{Me}_3[9]\text{aneN}_3)\text{R}]^+$ suggests the possibility of forming a dative $\text{N} \rightarrow \text{Al}$ bond, as has been found for the labile adduct $\text{Ti}(\eta\text{-C}_8\text{H}_8)(\mu\text{-N}^i\text{Bu})(\mu\text{-Me})\text{AlMe}_2$ (formed by reaction of $\text{Ti}(\eta\text{-C}_8\text{H}_8)(\text{N}^i\text{Bu})$ with TMA).⁷⁷ The relevant model species is **V-TIBA**, which had a formation energy of $-103.8 \text{ kJ mol}^{-1}$. The analogous TMA adduct (**V-TMA**) had a formation energy of $-136.1 \text{ kJ mol}^{-1}$.⁷⁵ Model **VI**, which is an isomer of **V-TIBA** but with the smaller methyl group in the $\text{Ti}(\mu\text{-CH}_2\text{R})\text{Al}$ linkage, was 11.1 kJ mol^{-1} more stable than **V-TIBA**, consistent with a reduction in steric pressure in the bridging unit.

In terms of electronic preferences, the calculations shown that simultaneous bonding of TIBA to the $\text{Ti}-\text{R}'$ and $\text{Ti}=\text{NR}$ groups of $[\text{Ti}(\text{NR})(\text{Me}_3[9]\text{aneN}_3)\text{R}]^+$ (cf. **V-TIBA**) would provide a greater stabilizing effect than forming two μ -alkyl bridges (cf.

(75) Bolton, P. D.; Clot, E.; Cowley, A. R.; Mountford, P. *J. Am. Chem. Soc.*, accepted for publication.

(76) Klimpel, M. G.; Eppinger, J.; Sirsch, P.; Scherer, W.; Anwander, R. *Organometallics* **2002**, *21*, 4021.

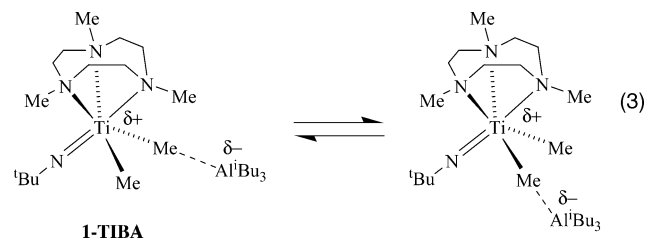
(77) Dunn, S. C.; Hazari, N.; Cowley, A. R.; Green, J. C.; Mountford, P. *Organometallics* **2006**, *25*, 1755.

IV-TIBA). This in turn would lead to a lower fraction of the metal centers being active for olefin polymerization. Such N-adducts would be very sensitive to the steric bulk at the imido nitrogen. Note also that while both model N→Al adducts **V** are more stable than their bis(μ -alkyl) counterparts **IV**, the stability gain in **V-TIBA** (-23.6 kJ mol $^{-1}$) is significantly less than in **V-TMA** (-37.7 kJ mol $^{-1}$). Since the real TMA adduct [Ti(N^tBu)(Me₃[9]aneN₃)(μ -Me)₂AlMe₂]⁺ does not contain a N_{imido}→Al interaction, it is unlikely that adducts of the type **V-TIBA** would form for sterically encumbered imido ligands. Moreover, bis(μ -alkyl) adducts of the type **IV** with TIBA should also be at least ca. 20 kJ mol $^{-1}$ enthalpically less stable than their TMA counterparts.⁷⁶

Overall, the DFT calculations find that both types of TIBA adduct may be accessible to varying degrees (depending on steric factors) in the experimental catalyst systems Ti(NR)(Me₃[9]aneN₃)R'₂/TB/TIBA. Bis(μ -alkyl) species would provide catalytically inactive resting states and/or intermediates on the pathway to chain transfer to TIBA, while N→Al adducts (for small imido R-groups) would also represent inactive/dormant species.

Reactions of Ti(NR)(Me₃[9]aneN₃)R'₂ with TIBA. At first sight, the structure–productivity trends for the dimethyl catalyst systems Ti(NR)(Me₃[9]aneN₃)Me₂/TB/TIBA could be adequately explained in terms of steric protection of the active species “[Ti(NR)(Me₃[9]aneN₃)R']⁺” (R' = polymeryl) toward the formation of heterobimetallic TIBA adducts (cf. Figure 5) and/or imido-bridged homobimetallic species [Ti₂(μ -NR)₂(Me₃[9]aneN₃)₂(R')₂]²⁺ (cf. dimeric **14**²⁺ vs monomeric²² [Ti(N^tBu)(Me₃[9]aneN₃)R']⁺). Similar explanations could be advanced for the Ti(NR)(Me₃[9]aneN₃)Cl₂/MAO²³ and related²⁵ catalyst systems.

However, the very contrasting productivities for the equally sterically protected *tert*-butyl imides Ti(N^tBu)(Me₃[9]aneN₃)R₂ (R = Me (**1**) ≫ CH₂SiMe₃ (**3**) ≈ CH₂Ph (**5**)), which differ only in the identity of the precatalyst Ti–R groups, show that this is not the only factor to consider. In these three systems, the catalytically active species ultimately formed should be effectively the same in each case after the first ethene insertions and/or chain transfer event. Furthermore, although the first-formed cations [Ti(N^tBu)(Me₃[9]aneN₃)R]⁺ (all instantly produced with TB) have nonclassical interactions that provide differing degrees of stabilization (modeled by **I-Me**, **I-CH₂SiMe₃**, and **I-CH₂Ph**), the NMR tube experiments between TIBA and [Ti(N^tBu)(Me₃[9]aneN₃)Me]⁺ and [Ti(N^tBu)(Me₃[9]aneN₃)-CH₂SiMe₃]⁺ showed both these cations react rapidly to exchange the precatalyst Ti–R groups. Therefore an “initiator effect” based on the ease of formation or stability of the first-formed [Ti(N^tBu)(Me₃[9]aneN₃)R]⁺ cations also appears to be ruled out. These questions, and the observation that **1**/TIBA alone (Table 3, entry 15) also forms a productive catalyst system, prompted us to examine the reactions of representative dialkyls Ti(NR)(Me₃[9]aneN₃)Me₂ with TIBA.



The ¹H NMR spectrum of a mixture of Ti(N^tBu)(Me₃[9]aneN₃)Me₂ (**1**) with TIBA (1 equiv) in C₆D₆ or C₆D₅Br showed

resonances for a single C_s symmetric titanium species containing a macrocycle, *tert*-butyl imido, and titanium-bound methyl ligands and a single isobutyl environment. The spectrum was reminiscent of the separated **1** and TIBA in the respective solvents, but the shifts clearly differed, indicative of an interaction between the two compounds. Cooling the C₆D₅Br solution to -30 °C resulted in broadening of the resonances. The NMR spectra are consistent with a “cation-like”⁷⁸ weak adduct of the type Ti(N^tBu)(Me₃[9]aneN₃)Me(μ -Me)AlⁱBu₃ (**1-TIBA**), which is still in the fast-exchange regime at -30 °C (eq 3). As drawn, **1-TIBA** is an analogue of the well-established zwitterions L_nMMe(μ -Me)BAR^F₃, which are sometimes formed when dimethyl complexes are activated with BAR^F₃.^{30,78,79} Compound **1-TIBA** may be considered as a “masked” form of [Ti(N^tBu)(Me₃[9]aneN₃)Me]⁺ stabilized by a polarizable and coordinating [AlⁱBu₃Me][−] anion. Strong anion coordination quenches the polymerization capability of Ziegler catalysts.^{30,32} Therefore, although the catalyst system **1**/TIBA has some productivity, it is only in the presence of TB that a very good catalyst system is formed. The origin of the bimodal molecular weight distribution in this case is not clear. The reaction of **1-TIBA** with TB is described below.

NMR tube scale reactions were also carried out between Ti(N^tBu)(Me₃[9]aneN₃)R₂ (R = CH₂SiMe₃ (**3**) or CH₂Ph (**5**)) and TIBA (1 equiv) in C₆D₆. Each immediately formed ill-defined and complex mixtures, with sets of resonances for several macrocycle, *tert*-butyl, and isobutyl environments. This behavior of **3** and **5** is in stark contrast to the clean formation of **1-TIBA** in the case of the dimethyl homologue **1**. Further reactions were carried out between TIBA (1 equiv) and Ti(NPh)(Me₃[9]aneN₃)Me₂ (**7**) or Ti(N-2,6-C₆H₃Pr₂)(Me₃[9]aneN₃)Me₂ (**9**), both poorly or unproductive precatalysts, and also Ti(N-2-C₆H₄Bu)(Me₃[9]aneN₃)Me₂ (**11**), the only other highly productive compound in Table 3. Like **3** and **5**, compounds **7** and **9** gave complex mixtures with TIBA in C₆D₆. In contrast, the ¹H NMR spectrum of the 1:1 mixture of **11** and TIBA was well-defined, showing resonances for the two components that were somewhat shifted from their positions prior to reaction. For completeness we also examined the reaction between the phenyl imido dichloride Ti(NPh)(Me₃[9]aneN₃)Cl₂²³ and TIBA (1 equiv), in order to confirm that it is the Ti–Me bonds of **7** (rather than the imido or macrocyclic ligands) that react. In contrast to the complex mixture formed between **7** and TIBA, no reaction occurred in the case of Ti(NPh)(Me₃[9]aneN₃)Cl₂. Overall these results suggest that the low polymerization productivity of many of the compounds in Table 1 might in part be attributable to unfavorable reactions between the precatalyst Ti–alkyl bonds and the TIBA.

Role of TIBA in the Catalyst Activation Process for 1. Transition metal isobutyl compounds undergo hydride abstraction with [Ph₃C]⁺, forming Ph₃CH, isobutene, and polymerization-active cations.^{61,65} However, this is not a likely activation process for **1**/TIBA since **1** did not undergo any detectable Ti–Me/Al–iBu group exchange on the NMR tube scale even after extended periods.⁸⁰ However, it is known that TB rapidly reacts with TIBA at ambient temperature via hydride abstraction to form Ph₃CH, isobutene, and “[AlⁱBu₂]⁺”.⁶⁴ The aluminum cation subsequently reacts with [BAR^F₄][−], giving mixtures of Al(ⁱBu)_x–

(78) Yang, X.; Stern, C. L.; Marks, T. J. *J. Am. Chem. Soc.* **1991**, *113*, 3623.

(79) Piers, W. E. *Adv. Organomet. Chem.* **2005**, *52*, 1.

(80) We cannot rule out the possibility of a small degree of alkyl group exchange between Ti and Al at the high ratios used in the polymerization experiments.

(Ar^F)_y and B(^tBu)_x(Ar^F)_y ($x + y = 3$). Similar chemistry has been reported for the anilinium borate [PhNMe₂H][BAR^F₄].⁶³

As we have shown, reaction of Ti(N^tBu)(Me₃[9]aneN₃)Me₂ (**1**) with TB quantitatively gives the methyl cation [Ti(N^tBu)(Me₃[9]aneN₃)Me]⁺ and the trityl derivative Ph₃CMe.^{20,22} In the presence of TMA (1 equiv), methide abstraction also occurs, forming Ph₃CMe and [Ti(N^tBu)(Me₃[9]aneN₃)(μ-Me)₂AlMe₂]⁺.²¹ However, it was not apparent what the equivalent activation reaction of **1** with TB would be in the presence of TIBA, and so a further NMR tube scale experiment was carried out. Reaction of TB (1 equiv) with a 1:1 mixture of **1** and TIBA in C₆D₅Br immediately gave complete consumption of all of the starting materials. The ¹H spectrum in the δ 3.5 to -0.5 ppm region was reminiscent of the mixture formed in the reaction between [Ti(N^tBu)(Me₃[9]aneN₃)Me]⁺ and TIBA (Scheme 2) with some sets of resonances apparently in common. Most importantly, the *only* trityl-derived product observed was Ph₃CH. This was formed in essentially quantitative yield, as judged against an internal toluene standard (comparing Ph₃CH and PhMe) resonances. There was no detectable Ph₃CMe, which would have arisen from methide abstraction from **1**. The ¹⁹F NMR spectrum of the mixture showed a single set of resonances for the [BAR^F₄]⁻ anion and none for the redistribution products Al(^tBu)_x(Ar^F)_y or B(^tBu)_x(Ar^F)_y.^{63,64}

These results are interesting since they suggest that β-hydride abstraction from TIBA (free or weakly coordinated as **1**·TIBA (eq 3)) is considerably more favored than methide abstraction, even at a 1:1 Al:Ti molar ratio (in the polymerization experiments a 2500:1 ratio was used). The implication is that the first-formed cation in the **1**/TB/TIBA catalyst system is of the type [Ti(N^tBu)(Me₃[9]aneN₃)(μ-Me)₂Al^tBu₂]⁺, formally derived from addition of “[Al^tBu₂]⁺” to **1**. Further equilibria arising from this species (e.g., via alkyl group redistribution and/or β-H elimination from monomeric species of the type **II** in Scheme 2) would help explain the appearance of the ¹H NMR spectra of the reaction mixture. Unsurprisingly, admission of ethylene (1.1 bar) to the NMR tube containing the **1**/TB/TIBA mixture produced a precipitate of polyethylene. We note that Götz and co-workers have proposed a role for “[Al^tBu₂]⁺” in TIBA/anilinium borate-activated zirconocene catalyst systems, although this case involved hydride abstraction from an isobutyl ligand.⁶³

Conclusions

We have developed synthetic routes to a range of macrocycle-supported imido titanium dialkyl compounds and determined a number of their X-ray structures. These compounds are generally less thermally and light sensitive than their isolobal titanocene analogues. A number of them form single site-type ethylene polymerization catalysts on activation with TB in the presence of TIBA. The structure–productivity trends for the dimethyl precatalysts vary as a function of imido substituent and parallel those of the dichloride-based Ti(NR)(Me₃[9]aneN₃)Cl₂/MAO family reported before.²³

In the Ti(NR)(Me₃[9]aneN₃)Me₂/TB/TIBA catalysts the TIBA acts both as a scavenger and as a chain transfer reagent, forming isobutyl cations, which readily undergo β-H transfer in either stoichiometric or catalytic contexts. DFT calculations indicated that TIBA, although it is a rather bulky aluminum alkyl, is able to form adducts with imido titanium alkyl cations and that the stability and type of adduct formed will depend on the steric properties of the imido substituent. The outcomes of the reactions between the various Ti(NR)(Me₃[9]aneN₃)R'₂ species and TIBA appeared to broadly parallel the polymerization capabilities of the associated catalyst systems. Thus the precatalysts

giving poor polymerization productivity also form a number of different and unknown products on exposure to TIBA. Since TB reacts preferentially with TIBA to **1**, forming Ph₃CH, it appears that a transient “[Al^tBu₂]⁺” cation plays an important role in the activation of the titanium dialkyl species.

The adverse effects of aluminum alkyls on group 4 catalyst systems and their precursors are well known and involve the trapping of active species as well as (pre)catalyst decomposition and other detrimental pathways.^{30,35–44,81–90} Therefore, in the catalyst systems reported here, the imido group appears to have two roles: (i) to stabilize the dialkyl precatalyst to degradation by the TIBA itself and (ii) to inhibit the formation of catalytically inactive heterobimetallic or homobimetallic complexes.

Experimental Section

General Methods and Instrumentation. All manipulations were carried out using standard Schlenk line or drybox techniques under an atmosphere of argon or of dinitrogen. Protio- and deuteriosolvents were predried over activated 4 Å molecular sieves and were refluxed over the appropriate drying agent, distilled, and stored under dinitrogen in Teflon valve ampules. NMR samples were prepared under dinitrogen in 5 mm Wilmad 507-PP tubes fitted with J. Young Teflon valves. ¹H, ¹³C{¹H}, ¹⁹F, and ²⁹Si NMR spectra were recorded on Varian Mercury-VX 300 and Varian Unity Plus 500 spectrometers. ¹H and ¹³C assignments were confirmed when necessary with the use of DEPT-135, DEPT-90, and two-dimensional ¹H–¹H and ¹³C–¹H NMR experiments. ¹H and ¹³C spectra were referenced internally to residual protiosolvent (¹H) or solvent (¹³C) resonances and are reported relative to tetramethylsilane (δ = 0 ppm). ¹⁹F and ²⁹Si spectra were referenced externally to CFC₃ and tetramethylsilane, respectively. Chemical shifts are quoted in δ (ppm) and coupling constants in Hertz. Infrared spectra were prepared as Nujol mulls between KBr or NaCl plates and were recorded on Perkin-Elmer 1600 and 1710 series FTIR spectrometers. Infrared data are quoted in wavenumbers (cm⁻¹). Mass spectra were recorded by the mass spectrometry service of Oxford University's Department of Chemistry. Elemental analyses were carried out by the analytical laboratory of the School of Chemistry, University of Nottingham, Inorganic Chemistry Laboratory, University of Oxford, or Elemental Analysis Service at the London Metropolitan University. GPC analyses were carried out by Rapra Technology Ltd. in 1,2,4-trichlorobenzene solvent at 160 °C relative to polystyrene calibrants and using the appropriate Mark Houwink parameters for polyethylene.

Starting Materials. The compounds Ti(NR)(Me₃[9]aneN₃)Cl₂,²³ LiCH₂SiMe₃,⁹¹ and LiCH₂Bu,⁹² were prepared according to the

(81) Zhu, F.; Huang, Q.; Lin, S. *J. Polym. Sci., Part A: Polym. Chem.* **1999**, *37*, 4497.

(82) Chien, J. C. W.; Salajka, Z.; Dong, S. *Macromolecules* **1992**, *25*, 3199.

(83) Zhu, F.; Huang, Y.; Yang, Y.; Lin, S. *J. Polym. Sci., Part A: Polym. Chem.* **2000**, *38*, 4258.

(84) Kickham, J. E.; Guerin, F.; Stephan, D. W. *J. Am. Chem. Soc.* **2002**, *124*, 11486.

(85) Kickham, J. E.; Guerin, F.; Stewart, J. C.; Stephan, D. W. *Angew. Chem., Int. Ed.* **2000**, *39*, 3263.

(86) Kickham, J. E.; Guerin, F.; Stewart, J. C.; Urbanska, E.; Ong, C. M.; Stephan, D. W. *Organometallics* **2001**, *20*, 1175.

(87) Kickham, J. E.; Guerin, F.; Stewart, J. C.; Urbanska, E.; Ong, C. M.; Stephan, D. W. *Organometallics* **2001**, *20*, 3209.

(88) Kretschmer, W. P.; Dijkhuis, C.; Meetsma, A.; Hessen, B.; Teuben, J. H. *Chem. Comm.* **2002**, 608.

(89) Stapleton, R. A.; Galan, B. R.; Collins, S.; Simons, R. S.; Garrison, J. C.; Youngs, W. J. *J. Am. Chem. Soc.* **2003**, *125*, 9246.

(90) Busico, V.; Cipullo, R.; Cutillo, F.; Friederichs, N.; Ronca, S.; Wang, B. *J. Am. Chem. Soc.* **2003**, *125*, 12402.

(91) Tessier-Youngs, C.; Beachley, O. T. *Inorg. Synth.* **1986**, *24*, 95.

(92) Davidson, P. J.; Lappert, M. F.; Pearce, R. *J. Organomet. Chem.* **1973**, *57*, 269.

literature methods. Other reagents were purchased and used without further purification.

Ti(NⁱBu)(Me₃[9]aneN₃)Me₂ (1). Methyl lithium (3.05 mL, 1.6 M in Et₂O, 4.87 mmol) was added to a vigorously stirred suspension of Ti(NⁱBu)(Me₃[9]aneN₃)Cl₂ (0.800 g, 2.21 mmol) in THF (30 mL) at -78 °C. The reaction mixture was allowed to warm very slowly to room temperature and then stirred for 16 h. The volatiles were removed under reduced pressure to give a yellow solid. The solid was extracted into benzene (20 mL) and filtered, and the volatiles were removed under reduced pressure. The resulting yellow solid was dissolved in a mixture of hexane and benzene (20 mL: 10 mL), filtered to remove undissolved material, and cooled to -30 °C for 1 day to give **1** as yellow crystals. Yield: 0.500 g (70%). Diffraction-quality crystals were grown from a saturated benzene/hexane solution at -30 °C. ¹H NMR (C₆D₆, 300.1 MHz, 298 K): 2.65 (6H, s, NMe *cis*), 2.52 (2H, m, CH₂), 2.43 (3H, s, NMe *trans*), 2.35 (2H, m, CH₂), 2.19 (2H, m, CH₂), 1.69 (2H, m, CH₂), 1.66 (2H, m, CH₂), 1.65 (9H, s, NCMe₃), 1.61 (2H, m, CH₂), 0.36 (6H, s, TiMe). ¹³C{¹H} NMR (C₆D₆, 75.5 MHz, 298 K): 64.7 (NCMe₃), 55.5 (CH₂), 55.1 (CH₂), 54.8 (CH₂), 51.8 (NMe *cis*), 48.5 (NMe *trans*), 33.5 (NCMe₃), 26.4 (TiMe). IR (NaCl plates, Nujol mull, cm⁻¹): 2920 (s), 2853 (s), 1495 (m), 1364 (m), 1343 (m), 1299 (m), 1245 (s), 1204 (s), 1151 (m), 1117 (m), 1099 (m), 1008 (s), 993 (m), 891 (m), 777 (s), 747 (m). FI-MS: *m/z* 320.3 (12%) [M]⁺, 305.3 (100%) [M - Me]⁺. Anal. Found (calcd for C₁₅H₃₆N₄Ti): C 56.2 (56.2), H 11.2 (11.3), N 17.4 (17.5).

Ti(NⁱBu)(Me₃[9]aneN₃)(Cl)Me (2). Methyl lithium (0.62 mL, 1.6 M in Et₂O, 1.00 mmol) was added to a stirred suspension of Ti(NⁱBu)(Me₃[9]aneN₃)Cl₂ (0.361 g, 1.00 mmol) in tetrahydrofuran (20 mL) at -78 °C and in the absence of light. The reaction mixture was allowed to warm slowly to room temperature and then stirred for a further 16 h. The volatiles were removed under reduced pressure to give a yellow solid. The solid was extracted into benzene (20 mL) and filtered, and the solution concentrated to approximately 5 mL. The product was then cautiously precipitated by the slow addition of pentane (25 mL) with vigorous stirring. The resulting yellow precipitate was filtered off, washed with pentane (3 × 5 mL), and dried in vacuo to give **2** as a pale yellow powder. Yield: 0.186 g (55%). ¹H NMR (C₆D₆, 300.1 MHz, 298 K): 2.92 (3H, s, NMe *cis*), 2.73 (3H, m, CH₂), 2.71 (3H, s, NMe *cis*), 2.59 (3H, s, NMe *trans*), 2.27 (3H, m, CH₂), 2.03 (2H, m, CH₂), 1.89 (4H, overlapping m, CH₂), 1.50 (9H, s, NCMe₃), 0.75 (3H, s, TiMe). ¹³C{¹H} NMR (C₆D₆, 75.5 MHz, 298 K): 66.9 (NCMe₃), 56.7 (CH₂), 55.8 (CH₂), 55.5 (CH₂), 55.3 (2 × CH₂), 54.6 (CH₂), 53.0 (NMe *cis*), 52.8 (NMe *cis*), 49.2 (NMe *trans*), 33.4 (TiMe), 32.5 (NCMe₃). IR (NaCl plates, Nujol mull, cm⁻¹): 2920 (s), 2854 (s), 1497 (m), 1347 (m), 1298 (m), 1249 (s), 1205 (m), 1155 (m), 1121 (w), 1008 (s), 993 (m), 893 (w), 780 (m), 747 (m). FI-MS: *m/z* 340.2 (70%) [M]⁺, 325.2 (100%) [M - Me]⁺, 171.2 (15%) [Me₃[9]aneN₃]⁺. FI-HRMS: *m/z* found (calcd for C₁₄H₃₃ClN₄Ti, [M]⁺) 340.1857 (340.1873). Anal. Found (calcd for C₁₄H₃₃ClN₄Ti): C 48.6 (49.4), H 9.6 (9.8), N 16.3 (16.4). The low %C may be attributed to the presence of trace amounts of the Ti(NⁱBu)(Me₃[9]aneN₃)Cl₂ starting material.

Ti(NⁱBu)(Me₃[9]aneN₃)(CH₂SiMe₃)₂ (3). Cold benzene (60 mL) was added to a mixture of Ti(NⁱBu)(Me₃[9]aneN₃)Cl₂ (0.361 g, 1.00 mmol) and LiCH₂SiMe₃ (0.188 g, 2.00 mmol) at 5 °C with vigorous stirring and in the absence of light. The orange suspension was allowed to warm to room temperature and then stirred for 17 h. The resulting deep yellow, cloudy solution was filtered to remove suspended material, and then the volatiles were removed under reduced pressure to give a yellow-brown semisolid. The product was extracted into the minimum pentane (35 mL) and cooled first to -25 °C for 24 h and then to -80 °C for 2 days to give **3** as bright yellow crystals. Yield: 0.336 g (72%). ¹H NMR (C₆D₆, 300.1 MHz, 298 K): 2.65 (6H, s, NMe *cis*), 2.51 (2H, m, NCH₂), 2.28 (3H, s, NMe *trans*), 2.27 (2H, m, NCH₂), 2.24 (2H, m, NCH₂),

1.65 (2H, m, NCH₂), 1.62 (2H, m, NCH₂), 1.58 (2H, m, NCH₂), 1.51 (9H, s, NCMe₃), 0.49 (18H, s, CH₂SiMe₃), 0.42 (2H, d, ²J 10.4 Hz, CH_aH_bSiMe₃), -0.19 (2H, d, ²J 10.4 Hz, CH_aH_bSiMe₃). ¹³C{¹H} NMR (C₆D₆, 75.5 MHz, 298 K): 66.1 (NCMe₃), 56.0 (NCH₂), 55.3 (NCH₂), 55.1 (NCH₂), 52.6 (NMe *cis*), 49.4 (NMe *trans*), 41.6 (CH₂SiMe₃), 33.8 (NCMe₃), 4.7 (CH₂SiMe₃). ²⁹Si NMR (HMQC ¹H-observed, CD₂Cl₂, 299.9 MHz, 293 K): -1.8 (CH₂SiMe₃). ²⁹Si NMR (HMQC ¹H-observed, C₆D₅Br, 299.9 MHz, 293 K): -3.1 (CH₂SiMe₃). IR (KBr pellet, cm⁻¹): 2816 (br s), 1494 (m), 1464 (s), 1366 (w), 1346 (m), 1300 (m), 1236 (s), 1202 (m), 1152 (m), 1112 (m), 1082 (s), 1070 (s), 1010 (s), 884 (s), 850 (s), 816 (s), 776 (m), 748 (s), 730 (s), 666 (m), 588 (m), 528 (m), 410 (m). Anal. Found (calcd for C₂₁H₅₂N₄Si₂Ti): C 52.6 (54.3), H 11.4 (11.3), N 11.8 (12.1). The low %C is attributed to titanium carbide formation.

Ti(NⁱBu)(Me₃[9]aneN₃)(CH₂ⁱBu)₂ (4). Cold benzene (60 mL) was added to a mixture of Ti(NⁱBu)(Me₃[9]aneN₃)Cl₂ (0.361 g, 1.00 mmol) and LiCH₂ⁱBu (0.156 g, 2.00 mmol) at 5 °C with vigorous stirring and in the absence of light. The orange suspension was allowed to warm to room temperature and then stirred for 17 h. An aliquot was taken, and the ¹H NMR spectrum showed that the reaction mixture contained a 1:3 mixture of the desired product to a monoalkylated species. Therefore a further 0.10 g (1.3 mmol) of LiCH₂ⁱBu was added to the reaction mixture. The reaction mixture was stirred for a further 17 h. The resulting deep yellow, cloudy solution was filtered to remove suspended material, and then the volatiles were removed under reduced pressure to give a yellow-brown solid. The product was extracted into hexane (60 mL), and the volatiles were removed under reduced pressure to give **4** as a yellow powder. Yield: 0.086 g (20%). ¹H NMR (C₆D₆, 300.1 MHz, 293 K): 2.67 (6H, s, NMe *cis*), 2.42 (2H, m, NCH₂), 2.31 (3H, s, NMe *trans*), 2.31-2.18 (4H, overlapping m, NCH₂), 1.71 (18H, s, CH₂CMe₃), 1.63 (9H, s, NCMe₃), 1.63-1.48 (6H, overlapping m, NCH₂), 0.80 (2H, d, ²J 11.7 Hz, CH_aH_bCMe₃), 0.58 (2H, d, ²J 11.7 Hz, CH_aH_bCMe₃). ¹³C{¹H} NMR (C₆D₆, 75.4 MHz, 293 K): 78.0 (CH₂CMe₃), 67.0 (CH₂CMe₃), 57.7 (NCMe₃), 55.9 (NCH₂), 55.7 (NCH₂), 55.5 (NCH₂), 52.7 (NMe *cis*), 49.6 (NMe *trans*), 37.0 (CH₂CMe₃), 35.2 (NCMe₃). IR (NaCl plates, Nujol mull, cm⁻¹): 2924 (s), 2854 (s), 1492 (m), 1346 (m), 1301 (m), 1260 (w), 1237 (s), 1219 (s), 1201 (s), 1152 (m), 1126 (w), 1100 (m), 1083 (m), 1073 (m), 1011 (s), 889 (w), 797 (w), 773 (m), 749 (m). Anal. Found (calcd for C₂₃H₅₂N₄Ti): C 63.7 (63.9), H 12.2 (12.1), N 12.8 (13.0).

Ti(NⁱBu)(Me₃[9]aneN₃)(CH₂Ph)₂ (5). Benzylmagnesium chloride (2.00 mL, 1.0 M in Et₂O, 2.00 mmol) was added to a stirred solution of Ti(NⁱBu)(Me₃[9]aneN₃)Cl₂ (0.361 g, 1.00 mmol) in THF (50 mL) at -45 °C and in the absence of light. The resulting bright yellow solution was allowed to slowly warm to room temperature and then stirred for a further 20 h. 1,4-Dioxane (0.5 mL, 5.9 mmol) was added to the solution with stirring, resulting in a slight cloudiness. The volatiles were removed under reduced pressure to give a pale yellow solid. The product was extracted into toluene (120 mL) and the solution then filtered and the volume reduced to approximately 50 mL. The product was then cautiously precipitated by the slow addition of hexane (100 mL) with vigorous stirring. The resulting yellow precipitate was filtered off and dried under reduced pressure to give **5** as a bright yellow powder. Yield: 0.406 g (86%). ¹H NMR (C₆D₆, 300.1 MHz, 298 K): 7.41 (4H, d, ³J 7.3 Hz, 2-C₆H₅), 7.32 (4H, app. t, app. ³J 7.6 Hz, 3-C₆H₅), 6.91 (2H, t, ³J 7.2 Hz, 4-C₆H₅), 2.89 (2H, d, ²J 9.2 Hz, CH_aH_bPh), 2.46 (6H, s, NMe *cis*), 2.43 (2H, d, ²J 9.2 Hz, CH_aH_bPh), 2.38 (2H, m, NCH₂), 2.09 (2H, m, NCH₂), 2.08 (2H, m, NCH₂), 2.02 (3H, s, NMe *trans*), 1.51 (2H, m, NCH₂), 1.50 (2H, m, NCH₂), 1.48 (2H, m, NCH₂), 1.29 (9H, s, NCMe₃). ¹³C{¹H} NMR (C₆D₆, 75.5 MHz, 298 K): 158.0 (1-CH₂Ph), 127.7 (3-CH₂Ph), 125.8 (2-CH₂Ph), 118.2 (4-CH₂Ph), 67.7 (NCMe₃), 61.1 (CH₂Ph), 55.9 (NCH₂), 55.2 (NCH₂), 55.0 (NCH₂), 52.0 (NMe *cis*), 49.0 (NMe *trans*), 33.0 (NCMe₃).

IR (NaCl plates, Nujol mull, cm^{-1}): 3060 (w), 2932 (s), 2853 (s), 1591 (s), 1346 (w), 1299 (m), 1241 (s), 1217 (s), 1174 (w), 1153 (w), 1114 (w), 1008 (s), 948 (s), 929 (m), 871 (w), 777 (m), 743 (s), 697 (s). Anal. Found (calcd for $\text{C}_{27}\text{H}_{44}\text{N}_4\text{Ti}$): C 67.4 (68.6), H 9.3 (9.4), N 11.7 (11.9). The low %C is attributed to incomplete combustion (TiC formation).

Ti(NⁱPr)(Me₃[9]aneN₃)Me₂ (6). Methyl lithium (1.80 mL, 1.6 M in Et₂O, 2.88 mmol) was added slowly to a stirred suspension of Ti(NⁱPr)(Me₃[9]aneN₃)Cl₂ (500 mg, 1.44 mmol) in THF (60 mL) at -78°C . The reaction mixture was allowed to warm slowly to room temperature and stirred for 16 h. The volatiles were removed under reduced pressure and the resulting yellow-brown solid extracted into benzene (20 mL). Hexanes were added to induce crystallization, and the mixture was cooled to -30°C for 3 days. The solids were filtered off, washed with pentane (3×10 mL), and dried in vacuo to give a yellow-brown solid. Yield: 230 mg (52%). Diffraction-quality crystals were grown by cooling a subsaturated solution of **6** in benzene to 5°C . ¹H NMR (C₆D₆, 500.0 MHz, 293 K): 4.13 (1H, sept., ³J = 6.4 Hz, CHMe₂), 2.59 (6H, s, NMe *cis*), 2.41 (3H, s, NMe *trans*), 2.32 (2H, m, CH₂), 2.16 (2H, m, CH₂), 1.67 (4H, overlapping m, CH₂), 1.59 (4H, overlapping m, CH₂), 1.54 (6H, d, ³J = 6.4 Hz, CHMe₂), 0.34 (6H, s, TiMe). ¹³C{¹H} NMR (C₆D₆, 125.7 MHz, 293 K): 61.9 (CHMe₂), 55.4 (CH₂), 55.2 (CH₂), 54.7 (CH₂), 51.4 (NMe *cis*), 48.5 (NMe *trans*), 27.4 (CHMe₂), 26.1 (TiMe). IR (KBr plates, Nujol mull, cm^{-1}): 1496 (w), 1344 (w), 1298 (m), 1286 (m), 1260 (w), 1238 (s), 1208 (w), 1150 (w), 1130 (w), 1096 (m), 1078 (m), 1064 (m), 1008 (s), 990 (w), 892 (m), 778 (m), 746 (m), 722 (m), 642 (m), 580 (m), 512 (m), 444 (m). FI-MS: *m/z* 306.2 (68%) [M]⁺, 291.2 (100%) [M - Me]⁺, 171.2 (10%) [Me₃[9]aneN₃]⁺. FI-HRMS: *m/z* found (calcd for C₁₄H₃₄N₄Ti, [M]⁺) 306.2251 (306.2263). Surprisingly, a satisfactory combustional analysis could not be obtained.

Ti(NPh)(Me₃[9]aneN₃)Me₂ (7). Methyl lithium (1.97 mL, 1.6 M in Et₂O, 3.15 mmol) was added slowly to a stirred suspension of Ti(NPh)(Me₃[9]aneN₃)Cl₂ (600 mg, 1.57 mmol) in THF (70 mL) at -78°C . The reaction mixture was allowed to warm slowly to room temperature and stirred for 16 h. The volatiles were removed under reduced pressure, and the resulting yellow solid was extracted into toluene (200 mL). After 3 days at 4°C orange crystals of **7** had formed, which were filtered off and dried in vacuo. The mother liquor was concentrated to approximately 40 mL and cooled to 4°C for a further 3 days resulting in a second crop of crystals. Yield: 282 mg (53%). Diffraction-quality single crystals were grown by slow evaporation of a diethyl ether solution of **6**. ¹H NMR (C₆D₆, 499.9 MHz, 293 K): 7.35 (2H, dt, ³J 8.5 Hz, ⁴J 1.4 Hz, 2-C₆H₅), 7.31 (2H, app. t, app. ³J 7.7 Hz, 3-C₆H₅), 6.84 (1H, tt, ³J 7.2 Hz, ⁴J 1.5 Hz, 4-C₆H₅), 2.48 (3H, s, NMe *trans*), 2.45 (6H, s, NMe *cis*), 2.36–2.25 (4H, overlapping m, CH₂), 2.06 (2H, m, CH₂), 1.69 (2H, m, CH₂), 1.55–1.47 (4H, overlapping m, CH₂), 0.51 (6H, s, TiMe). ¹³C{¹H} NMR (C₆D₆, 125.7 MHz, 293 K): 160.8 (1-C₆H₅), 128.7 (2-C₆H₅), 124.0 (3-C₆H₅), 117.2 (4-C₆H₅), 55.7 (CH₂), 55.5 (CH₂), 54.7 (CH₂), 51.1 (NMe *cis*), 49.1 (NMe *trans*), 32.7 (TiMe). IR (NaCl plates, Nujol mull, cm^{-1}): 1575 (m), 1331 (s), 1159 (w), 1107 (w), 1063 (m), 1008 (m), 991 (m), 952 (w), 779 (w), 761 (m), 693 (w), 681 (w). FI-MS: *m/z* 340.2 (100%) [M]⁺, 325.2 (58%) [M - Me]⁺, 171.2 (40%) [Me₃[9]aneN₃]⁺. Anal. Found (calcd for C₁₇H₃₂N₄Ti): C 60.2 (60.0), H 9.4 (9.5), N 16.4 (16.5).

Ti(N-3,5-C₆H₃(CF₃)₂)(Me₃[9]aneN₃)Me₂ (8). Methyl lithium (1.81 mL, 1.6 M in Et₂O, 2.90 mmol) was added slowly to a stirred suspension of Ti(N-3,5-C₆H₃(CF₃)₂)(Me₃[9]aneN₃)Cl₂ (600 mg, 1.16 mmol) in THF (40 mL) at -78°C . The reaction mixture was allowed to warm slowly to room temperature and stirred for 16 h. The volatiles were removed under reduced pressure, and the resulting orange-brown solid was extracted into benzene (40 mL). The benzene solution was concentrated to approximately 30 mL and filtered away from some brown precipitate. The solution was further

concentrated to approximately 5 mL, and then the product was cautiously precipitated by the slow addition of pentane (20 mL) with vigorous stirring. The resulting orange precipitate was filtered off, washed with pentane (3×5 mL), and dried in vacuo to give **8** as an orange powder. Yield: 173 mg (31%). Diffraction-quality single crystals were grown by slow evaporation of a diethyl ether solution of **7**. ¹H NMR (C₆D₆, 499.9 MHz, 293 K): 7.70 (2H, s, 2-C₆H₃(CF₃)₂), 7.34 (1H, s, 4-C₆H₃(CF₃)₂), 2.41 (3H, s, NMe *trans*), 2.23 (2H, m, CH₂), 2.19 (6H, s, NMe *cis*), 2.05 (2H, m, CH₂), 1.90 (2H, m, CH₂), 1.61 (2H, m, CH₂), 1.42–1.35 (4H, overlapping m, CH₂), 0.45 (6H, s, TiMe). ¹³C{¹H} NMR (C₆D₆, 125.8 MHz, 293 K): 159.4 (1-C₆H₃(CF₃)₂), 131.9 (q, ²J_{C-F} 31.5 Hz, 3-C₆H₃(CF₃)₂), 125.0 (q, ¹J_{C-F} 273.0 Hz, CF₃), 123.0 (2-C₆H₃(CF₃)₂), 108.4 (4-C₆H₃(CF₃)₂), 57.5 (CH₂), 55.6 (CH₂), 55.2 (CH₂), 50.7 (NMe *cis*), 49.1 (NMe *trans*), 36.2 (TiMe). ¹⁹F NMR (C₆D₆, 282.2 MHz, 293 K): -67.7 (CF₃). IR (NaCl plates, Nujol mull, cm^{-1}): 1585 (m), 1397 (s), 1275 (s), 1166 (s), 1131 (s), 1115 (s), 1080 (w), 1062 (w), 1017 (s), 892 (w), 871 (w), 842 (w), 774 (m), 745 (w), 704 (w), 681 (m). FI-MS: *m/z* 460.9 (100%) [M - Me]⁺, 445.8 (18%) [M - 2Me]⁺, 229.0 (50%) [H₂N-3,5-(CF₃)₂C₆H₃]⁺, 171.2 (20%) [Me₃[9]aneN₃]⁺. Anal. Found (calcd for C₁₉H₃₀F₆N₄Ti): C 48.0 (47.9), H 6.4 (6.3), N 11.8 (11.8).

Ti(N-2,6-C₆H₃ⁱPr₂)(Me₃[9]aneN₃)Me₂ (9). Methyl lithium (1.61 mL, 1.6 M in Et₂O, 2.58 mmol) was added slowly to a stirred suspension of Ti(N-2,6-C₆H₃ⁱPr₂)(Me₃[9]aneN₃)Cl₂ (600 mg, 1.29 mmol) in THF (30 mL) at -78°C . The reaction mixture was allowed to warm slowly to room temperature and stirred for 16 h. The volatiles were removed under reduced pressure, and the resulting yellow solid was extracted into chlorobenzene (20 mL). The chlorobenzene solution was concentrated to approximately 5 mL and layered with pentane (10 mL). After 2 days at -30°C a yellow-brown precipitate had formed. This was filtered off and dissolved in THF (10 mL). The solution was concentrated to approximately 5 mL and cooled to -80°C for 5 days to give **9** as orange crystals. Yield: 206 mg (38%). Diffraction-quality single crystals were grown by slow diffusion of pentane into a toluene solution of **9**. ¹H NMR (C₆D₆, 499.9 MHz, 293 K): 7.28 (2H, d, ³J 7.6 Hz, 3-C₆H₃ⁱPr₂), 7.00 (1H, t, ³J 7.6 Hz, 4-C₆H₃ⁱPr₂), 4.84 (2H, sept., ³J 7.0 Hz, CHMe₂), 2.50 (2H, m, CH₂), 2.43 (6H, s, NMe *cis*), 2.42 (3H, s, NMe *trans*), 2.38 (2H, m, CH₂), 2.13 (2H, m, CH₂), 1.70–1.59 (4H, overlapping m, CH₂), 1.52 (2H, m, CH₂), 1.48 (12H, d, ³J 7.0 Hz, CHMe₂), 0.51 (6H, s, TiMe). ¹³C{¹H} NMR (C₆D₆, 125.7 MHz, 293 K): 156.5 (1-C₆H₃ⁱPr₂), 143.4 (2-C₆H₃ⁱPr₂), 123.2 (3-C₆H₃ⁱPr₂), 118.0 (4-C₆H₃ⁱPr₂), 56.2 (CH₂), 55.9 (CH₂), 55.5 (CH₂), 51.6 (NMe *cis*), 49.0 (NMe *trans*), 34.1 (TiMe), 27.5 (CHMe₂), 25.9 (CHMe₂). IR (NaCl plates, Nujol mull, cm^{-1}): 1582 (m), 1490 (w), 1415 (s), 1364 (m), 1355 (m), 1335 (s), 1273 (s), 1205 (w), 1153 (m), 1116 (m), 1101 (m), 1078 (m), 1067 (s), 1024 (m), 1007 (s), 954 (s), 891 (m), 778 (s), 754 (s). FI-MS: *m/z* 424.1 (4%) [M]⁺, 177.2 (21%) [H₂N-2,6-ⁱPr₂C₆H₃]⁺, 171.2 (100%) [Me₃[9]aneN₃]⁺. Anal. Found (calcd for C₂₃H₄₄N₄Ti): C 65.1 (65.1), H 10.4 (10.4), N 13.3 (13.2).

Ti(N-2-C₆H₄CF₃)(Me₃[9]aneN₃)Me₂ (10). Methyl lithium (1.72 mL, 1.6 M in Et₂O, 2.75 mmol) was added slowly to a stirred suspension of Ti(N-2-C₆H₄CF₃)(Me₃[9]aneN₃)Cl₂ (449 mg, 1.00 mmol) in THF (20 mL) at -78°C . The reaction mixture was allowed to warm slowly to room temperature and stirred for 16 h. The volatiles were removed under reduced pressure, and the resulting black semisolid was extracted into chlorobenzene (20 mL). The volatiles were removed, and the resulting yellow-brown solid was extracted into diethyl ether (140 mL), resulting in a bright yellow solution. The solution was concentrated to approximately 5 mL, and the resulting yellow precipitate was filtered off, washed with pentane (3×5 mL), and dried in vacuo to give **10** as a yellow powder. Yield: 79 mg (19%). ¹H NMR (C₆D₆, 499.9 MHz, 293 K): 8.14 (1H, d, ³J 8.3 Hz, 6-C₆H₄(CF₃)), 7.61 (1H, d, ³J 7.8 Hz, 3-C₆H₄(CF₃)), 7.28 (1H, app. t, app. ³J 7.7 Hz, 5-C₆H₄(CF₃)), 6.56

(1H, app. t, app. 3J 7.6 Hz, 4-C₆H₄(CF₃)), 2.54 (2H, m, CH₂), 2.44 (3H, s, NMe *trans*), 2.41 (6H, s, NMe *cis*), 2.31 (2H, m, CH₂), 2.02 (2H, m, CH₂), 1.69 (2H, m, CH₂), 1.57 (2H, m, CH₂), 1.52 (2H, m, CH₂), 0.53 (6H, s, TiMe). ¹³C{¹H} NMR (C₆D₆, 125.7 MHz, 293 K): 158.7 (1-C₆H₄(CF₃)), 133.5 (q, $^1J_{C-F}$ 307.8 Hz, CF₃), 133.4 (6-C₆H₄(CF₃)), 132.1 (5-C₆H₄(CF₃)), 125.6 (q, $^3J_{C-F}$ 6.1 Hz, 3-C₆H₄(CF₃)), 116.0 (q, $^2J_{C-F}$ 25.9 Hz, 2-C₆H₄(CF₃)), 115.4 (4-C₆H₄(CF₃)), 55.6 (CH₂), 55.2 (CH₂), 55.2 (CH₂), 50.7 (NMe *cis*), 49.2 (NMe *trans*), 37.3 (TiMe). ¹⁹F NMR (C₆D₆, 282.2 MHz, 293 K): -64.4 (CF₃). IR (NaCl plates, Nujol mull, cm⁻¹): 1590 (m), 1542 (w), 1445 (s), 1344 (s), 1317 (m), 1281 (w), 1219 (w), 1159 (w), 1107 (m), 1091 (m), 1048 (w), 1025 (m), 1007 (m), 951 (w), 779 (w). Anal. Found (calcd for C₁₈H₃₁F₃N₄Ti): C 53.1 (52.9), H 7.7 (7.7), N 13.0 (13.7).

Ti(N-2-C₆H₄^tBu)(Me₃[9]aneN₃)Me₂ (11). Methyl lithium (1.03 mL, 1.6 M in Et₂O, 1.65 mmol) was added slowly to a stirred suspension of Ti(N-2-C₆H₄^tBu)(Me₃[9]aneN₃)Cl₂ (360 mg, 0.82 mmol) in THF (30 mL) at -78 °C. The reaction mixture was allowed to warm slowly to room temperature and stirred for 16 h. The volatiles were removed under reduced pressure, and the resulting yellow solid was extracted into chlorobenzene (30 mL). The chlorobenzene solution was concentrated to approximately 5 mL, and then the product was cautiously precipitated by the slow addition of pentane (20 mL) with vigorous stirring. The resulting yellow precipitate was filtered off, washed with pentane (3 × 5 mL), and dried in vacuo to give **11** as a yellow powder. Yield: 188 mg (58%). Diffraction-quality single crystals were grown by slow diffusion of pentane into a benzene solution of **10**. ¹H NMR (C₆D₆, 499.9 MHz, 293 K): 7.58 (1H, dd, 3J 7.8 Hz, 4J 1.6 Hz, 3-C₆H₄^tBu), 7.25 (1H, app. td, 3J 7.6 Hz, 4J 1.6 Hz, 5-C₆H₄^tBu), 7.19 (1H, dd, 3J 8.1 Hz, 4J 1.5 Hz, 6-C₆H₄^tBu), 6.91 (1H, app. td, 3J 7.5 Hz, 4J 1.5 Hz, 4-C₆H₄^tBu), 2.53 (2H, m, CH₂), 2.45 (3H, s, NMe *trans*), 2.45 (6H, s, NMe *cis*), 2.30 (2H, m, CH₂), 2.16 (9H, s, CMe₃), 2.08 (2H, m, CH₂), 1.67 (2H, m, CH₂), 1.56 (2H, m, CH₂), 1.51 (2H, m, CH₂), 0.49 (6H, s, TiMe). ¹³C{¹H} NMR (C₆D₆, 125.7 MHz, 293 K): 160.1 (1-C₆H₄^tBu), 142.8 (2-C₆H₄^tBu), 129.1 (6-C₆H₄^tBu), 126.7 (3-C₆H₄^tBu), 125.7 (5-C₆H₄^tBu), 117.2 (4-C₆H₄^tBu), 55.9 (CH₂), 55.8 (CH₂), 55.3 (CH₂), 51.3 (NMe *cis*), 49.3 (NMe *trans*), 37.4 (TiMe), 36.6 (CMe₃), 31.2 (CMe₃). IR (NaCl plates, Nujol mull, cm⁻¹): 1578 (w), 1423 (m), 1297 (s), 1003 (m), 951 (m), 776 (w), 745 (m). FI-MS: *m/z* 396.5 (23%) [M]⁺, 171.2 (40%) [Me₃[9]aneN₃]⁺, 149.1 (100%) [H₂N-2-^tBuC₆H₄]⁺. Anal. Found (calcd for C₂₁H₄₀N₄Ti): C 63.5 (63.6), H 10.1 (10.2), N 14.0 (14.1).

Ti(NⁱPr)(Me₃[9]aneN₃)(CH₂SiMe₃)₂ (12). To an ice-cooled mixture of Ti(NⁱPr)(Me₃[9]aneN₃)Cl₂ (81 mg, 0.23 mmol) and LiCH₂-SiMe₃ (44 mg, 0.46 mmol) was added partially frozen benzene (20 mL) in the absence of light. The mixture was allowed to warm to room temperature and left to stir for a further 16 h in the dark. Subsequently the solids were filtered off to give a yellow solution. Removal of the volatiles under reduced pressure afforded **12** as a yellow powder. Yield: 40 mg (39%). ¹H NMR (C₆D₆, 499.9 MHz, 293 K): 4.25 (1H, sept, 3J 6.3 Hz, CHMe₂), 2.56 (6H, s, NMe *cis*), 2.38 (2H, m, NCH₂), 2.21 (3H, s, NMe *trans*), 2.17 (4H, overlapping m, NCH₂), 1.54 (6H, overlapping m, NCH₂), 1.33 (6H, d, 3J 6.3 Hz, CHMe₂), 0.53 (18H, s, CH₂SiMe₃), 0.03 (2H, d, 2J 11.2 Hz, CH_aH_bSiMe₃), -0.48 (2H, d, 2J 11.2 Hz, CH_aH_bSiMe₃). ¹³C{¹H} NMR (C₆D₆, 125.7 MHz, 293 K): 63.2 (CHMe₂), 55.8 (NCH₂), 55.2 (NCH₂), 55.1 (NCH₂), 52.3 (NMe *cis*), 49.3 (NMe *trans*), 41.0 (CH₂SiMe₃), 27.4 (CHMe₂), 4.7 (CH₂SiMe₃). IR (KBr plates, Nujol mull, cm⁻¹): 1492 (m), 1366 (m), 1297 (s), 1240 (w), 1221 (s), 1153 (m), 1126 (w), 1094 (w), 1087 (m), 1071 (m), 1059 (m), 1040 (m), 1008 (s), 966 (w), 913 (s), 888 (s), 879 (s), 853 (s), 810 (s), 774 (m), 745 (m), 724 (s), 679 (m), 662 (m), 618 (m), 574 (m), 511 (m), 495 (m), 450 (w), 411 (m). EI-MS: *m/z* 363 (35%) [M - CH₂SiMe₃]⁺. Anal. Found (calcd for C₂₀H₅₀N₄-Si₂Ti): C 53.1 (53.3), H 11.3 (11.2), N 12.2 (12.4).

Ti(NAr^F)(Me₃[9]aneN₃)(CH₂SiMe₃)₂ (13). To an ice-cooled mixture of Ti(NAr^F)(Me₃[9]aneN₃)Cl₂ (500 mg, 1.28 mmol) and LiCH₂SiMe₃ (240 mg, 2.56 mmol) was added partially frozen benzene (50 mL) in the absence of light. The mixture was allowed to warm to room temperature and left to stir for a further 16 h in the dark. Removal of the volatiles under reduced pressure afforded a brown oil, which was extracted into hot hexanes (5 × 10 mL) to give a yellow solution. The volatiles were removed under reduced pressure from the combined extracts to afford **13** as a yellow powder. Yield: 60 mg (8%). ¹H NMR (C₆D₆, 300.1 MHz, 293 K): 2.41 (6H, s, NMe *cis*), 2.39 (3H, s, NMe *trans*), 2.26 (4H, overlapping m, NCH₂), 2.06 (2H, m, NCH₂), 1.61 (6H, overlapping m, NCH₂), 0.77 (2H, d, 2J 11.0 Hz, CH_aH_bSiMe₃), 0.46 (18H, s, CH₂SiMe₃), 0.04 (2H, d, 2J 10.5 Hz, CH_aH_bSiMe₃). ¹³C{¹H} NMR (C₆D₆, 75.5 MHz, 293 K): 56.1 (NCH₂), 55.8 (NCH₂), 55.1 (NCH₂), 51.6 (NMe *cis*), 50.3 (NMe *trans*), 3.9 (CH₂SiMe₃). The C₆F₅ and CH₂SiMe₃ resonances were not observed. ¹⁹F NMR (C₆D₆, 282.4 MHz, 293 K): -153.6 (2F, dd, 3J 19.2 Hz, 4J 5.5 Hz, 2-C₆F₅), -168.5 (2F, app. t, app. 3J 21.9 Hz, 3-C₆F₅), -176.3 (1F, m, 4-C₆F₅). IR (KBr plates, Nujol mull, cm⁻¹): 1313 (m), 1235 (m), 1205 (m), 1155 (w), 1068 (w), 1035 (m), 1007 (m), 975 (m), 892 (m), 849 (m), 817 (m), 777 (m), 723 (m), 668 (w), 522 (w), 433 (w). EI-MS: *m/z* 487 (46%) [M - CH₂SiMe₃]⁺, 400 (65%) [M - 2CH₂SiMe₃]⁺. Anal. Found (calcd for C₂₃H₄₃F₅N₄Si₂Ti): C 48.1 (48.1), H 7.6 (7.6), N 9.6 (9.8).

[Ti₂(μ-NPh)₂(Me₃[9]aneN₃)₂Cl₂][BAR^F₄]₂ (14-BAR^F₄). To a solution of Ti(NPh)(Me₃[9]aneN₃)Me₂ (**7**, 50 mg, 0.147 mmol) in CH₂-Cl₂ (1 mL) was added [Ph₃C][BAR^F₄] (136 mg, 0.147 mmol) in CH₂Cl₂ (1 mL) to give a deep red solution. The solution was left to stand for 2 days, after which time some deep red-brown solid had formed. Pentane (2 mL) was added with stirring to precipitate more product, then the resulting dark red solid was filtered off, washed with pentane (3 × 1 mL), and dried in vacuo. Yield: 111 mg (74%). ¹H NMR (CD₂Cl₂, 499.9 MHz, 293 K): 7.15 (4H, app. t, app. 3J = 7.8 Hz, 3-C₆H₅), 7.00 (2H, t, 3J = 7.3 Hz, 4-C₆H₅), 6.81 (4H, d, 3J = 8.8 Hz, 2-C₆H₅), 3.78 (4H, m, CH₂), 3.42 (12H, s, NMe *cis*), 3.34 (4H, m, CH₂), 3.21 (4H, m, CH₂), 3.13 (4H, m, CH₂), 2.77-2.74 (8H, overlapping m, CH₂), 2.30 (6H, s, NMe *trans*). ¹³C{¹H} NMR (CD₂Cl₂, 75.5 MHz, 293 K): 158.0 (1-C₆H₅), 148.5 (br. d, $^1J_{C-F}$ = 238 Hz, 2-C₆F₅), 138.6 (br. d, $^1J_{C-F}$ = 247 Hz, 4-C₆F₅), 136.7 (br. d, $^1J_{C-F}$ = 250 Hz, 3-C₆F₅), 128.6 (3-C₆H₅), 126.0 (4-C₆H₅), 125.2 (2-C₆H₅), 57.5 (CH₂), 57.2 (CH₂), 54.5 (CH₂), 52.1 (NMe *cis*), 50.9 (NMe *trans*). ¹⁹F NMR (CD₂Cl₂, 282.1 MHz, 293 K): -133.5 (d, 3J = 10.6 Hz, 2-C₆F₅), -164.0 (t, 3J = 20.4 Hz, 4-C₆F₅), -167.9 (app. t, app. 3J = 18.1 Hz, 3-C₆F₅). IR (KBr plates, Nujol mull, cm⁻¹): 1643 (m), 1582 (w), 1514 (s), 1411 (w), 1295 (w), 1274 (m), 1222 (w), 1088 (s), 997 (m), 978 (s), 887 (w), 774 (m), 757 (m), 684 (m), 662 (m). Anal. Found (calcd for C₇₈H₅₂B₂Cl₂F₄₀N₈Ti₂): C 45.8 (45.7), H 2.7 (2.6), N 5.6 (5.5).

[Ti(NPh)(Me₃[9]aneN₃){MeC(NⁱPr)₂}] [BAR^F₄] (15-BAR^F₄). To a solution of Ti(NPh)(Me₃[9]aneN₃)Me₂ (**7**, 50 mg, 0.147 mmol) and ⁱPrNCNⁱPr (23 μL, 0.147 mmol) in CH₂Cl₂ (1 mL) at -35 °C was added [Ph₃C][BAR^F₄] (136 mg, 0.147 mmol) in CH₂Cl₂ (1 mL) to give a brown-yellow solution. The solution was concentrated to approximately 1 mL, then pentane (4 mL) was added with stirring, resulting in a brown-yellow oil. The supernatant was decanted and the oil triturated in pentane for 10 min to give **15-BAR^F₄** as a yellow powder, which was washed with pentane (3 × 1 mL) and dried in vacuo. Yield: 73 mg (44%). ¹H NMR (CD₂Cl₂, 299.9 MHz, 293 K): 7.04 (2H, app. t, app. 3J = 7.7 Hz, 3-C₆H₅), 6.76 (1H, t, 3J = 7.5 Hz, 4-C₆H₅), 6.72 (2H, d, 3J = 7.5 Hz, 2-C₆H₅), 4.10 (2H, app. sept., app. 3J = 6.8 Hz, CHMe₂), 3.82 (2H, m, CH₂), 3.26 (2H, m, CH₂), 3.19 (6H, s, NMe *cis*), 3.01-2.95 (4H, overlapping m, CH₂), 2.76 (2H, m, CH₂), 2.65 (2H, m, CH₂), 2.32 (3H, s, CMe₂), 2.29 (3H, s, NMe *trans*), 1.37 (6H, d, 3J = 6.8 Hz, CHMe₂), 1.33 (6H, d, 3J = 6.8 Hz, CHMe₂). ¹³C{¹H} NMR (CD₂Cl₂, 75.4 MHz, 293 K): 167.5 (CMe), 159.0 (1-C₆H₅), 148.5 (br. d, $^1J_{C-F}$ = 238 Hz,

Table 4. X-ray Data Collection and Processing Parameters for Ti(NR)(Me₃[9]aneN₃)Me₂·xC₆H₆ (R = ⁱBu (1·C₆H₆), ⁱPr (6·0.5C₆H₆), Ph (7), 3,5-C₆H₃(CF₃)₂ (8))

parameter	1·C ₆ H ₆	6·0.5C ₆ H ₆	7	8
empirical formula	C ₁₅ H ₃₆ N ₄ Ti·C ₆ H ₆	C ₁₄ H ₃₄ N ₄ Ti·0.5(C ₆ H ₆)	C ₁₇ H ₃₂ N ₄ Ti	C ₁₉ H ₃₀ F ₆ N ₄ Ti
fw	398.49	345.41	340.37	476.36
temp/K	150	150	150	150
wavelength/Å	0.71073	0.71073	0.71073	0.71073
space group	<i>P</i> 2 ₁ / <i>c</i>	<i>C</i> 2/ <i>c</i>	<i>P</i> 2 ₁ / <i>n</i>	<i>P</i> 2 ₁ 2 ₁ 2 ₁
<i>a</i> /Å	16.6168(3)	35.1006(8)	11.6320(4)	8.5573(2)
<i>b</i> /Å	9.0660(2)	8.3540(2)	13.6112(6)	14.1080(2)
<i>c</i> /Å	17.3742(4)	13.6754(4)	12.2864(6)	18.5066(2)
α/deg	90	90	90	90
β/deg	114.96(1)	95.7541(8)	103.7200(15)	90
γ/deg	90	90	90	90
<i>V</i> /Å ³	2373.0(2)	3989.8(2)	1889.75(14)	2234.23(7)
<i>Z</i>	4	8	4	4
<i>d</i> (calcd)/Mg m ⁻¹	1.115	1.150	1.196	1.416
abs coeff/mm ⁻¹	0.372	0.430	0.456	0.445
<i>R</i> indices ^a	<i>R</i> ₁ = 0.0506	<i>R</i> ₁ = 0.0417	<i>R</i> ₁ = 0.0449	<i>R</i> ₁ = 0.0414
[<i>I</i> > 3σ(<i>I</i>)]	<i>R</i> _w = 0.0617	<i>R</i> _w = 0.0238	<i>R</i> _w = 0.0544	<i>R</i> _w = 0.0487

$$^a R_1 = \sum(|F_o| - |F_c|)/\sum|F_o|; R_w = \sqrt{\sum w(|F_o| - |F_c|)^2/\sum w|F_o|^2}. wR_2 = \sqrt{\sum w(F_o^2 - F_c^2)^2/\sum w(F_o^2)^2}.$$

Table 5. X-ray Data Collection and Processing Parameters for Ti(NR)(Me₃[9]aneN₃)Me₂·xC₆H₆ (R = 2,6-C₆H₃ⁱPr₂ (9), 2-C₆H₄ⁱBu (11)) and [Ti(NPh)(Me₃[9]aneN₃){MeC(NⁱPr)₂}] [BAR^F₄]·CH₂Cl₂ (15-BAR^F₄·CH₂Cl₂)

parameter	9	11	15-BAR ^F ₄ ·CH ₂ Cl ₂
empirical formula	C ₂₃ H ₄₄ N ₄ Ti	C ₂₁ H ₄₀ N ₄ Ti	C ₄₇ H ₄₃ BF ₂₀ N ₆ Ti·CH ₂ Cl ₂
fw	424.53	396.48	1215.50
temp/K	150	150	150
wavelength/Å	0.71073	0.71073	0.71073
space group	<i>P</i> 2 ₁ / <i>c</i>	monoclinic	<i>P</i> 2 ₁ / <i>c</i>
<i>a</i> /Å	9.1367(3)	9.1367(3)	9.2576(2)
<i>b</i> /Å	16.2609(5)	16.2609(5)	15.0649(3)
<i>c</i> /Å	16.4873(5)	16.4873(5)	16.0266(3)
α/deg	90	90	90
β/deg	93.5206(16)	98.1573(11)	107.6272(10)
γ/deg	90	90	90
<i>V</i> /Å ³	2444.91(13)	2212.53(8)	5095.86(16)
<i>Z</i>	4	4	4
<i>d</i> (calcd)/Mg m ⁻¹	1.153	1.190	1.584
abs coeff/mm ⁻¹	0.365	0.399	0.389
<i>R</i> indices ^a	<i>R</i> ₁ = 0.0461	<i>R</i> ₁ = 0.0469	<i>R</i> ₁ = 0.0332
[<i>I</i> > 3σ(<i>I</i>)]	<i>R</i> _w = 0.0532	<i>R</i> _w = 0.0603	<i>R</i> _w = 0.0387

$$^a R_1 = \sum(|F_o| - |F_c|)/\sum|F_o|; R_w = \sqrt{\sum w(|F_o| - |F_c|)^2/\sum w|F_o|^2}. wR_2 = \sqrt{\sum w(F_o^2 - F_c^2)^2/\sum w(F_o^2)^2}.$$

2-C₆F₅), 138.6 (br d, ¹J_{C-F} = 247 Hz, 4-C₆F₅), 136.7 (br d, ¹J_{C-F} = 250 Hz, 3-C₆F₅), 128.7 (3-C₆H₅), 124.6 (2-C₆H₅), 121.9 (4-C₆H₅), 57.4 (CH₂), 56.1 (CH₂), 54.9 (CH₂), 51.3 (NMe *cis*), 50.6 (CHMe₂), 47.5 (NMe *trans*), 25.2 (CHMe₂), 24.6 (CHMe₂), 14.0 (CMe). ¹⁹F NMR (CD₂Cl₂, 282.1 MHz, 293 K): -133.5 (d, ³J = 10.6 Hz, 2-C₆F₅), -164.0 (t, ³J = 20.4 Hz, 4-C₆F₅), -167.9 (app. t, app. ³J = 18.1 Hz, 3-C₆F₅). IR (NaCl plates, Nujol mull, cm⁻¹): 1643 (m), 1581 (w), 1513 (s), 1413 (m), 1312 (m), 1275 (m), 1204 (m), 1177 (w), 1086 (s), 1002 (m), 979 (s), 775 (m), 757 (m), 684 (m), 662 (m). ES⁺MS (MeCN): *m/z* 451.3 (100%) [M]⁺, 143.1 (80%) [ⁱPrNHCMeNHⁱPr]⁺. ES⁺HRMS (MeCN): *m/z* found (calcd for C₂₃H₄₃N₆Ti, [M]⁺) 451.3018 (451.3029). Anal. Found (calcd for C₄₇H₄₃BF₂₀N₆Ti): C 49.8 (49.9), H 3.9 (3.8), N 7.6 (7.4).

Typical Procedure for Ethylene Polymerization Using TB and TIBA. All manipulations were carried out under ethylene (~1.1 bar) working gas. Stock solutions of Ti(NⁱBu)(Me₃[9]aneN₃)Me₂ (1, 6.4 mg, 20 μmol in 100 mL of toluene) and [Ph₃C][BAR^F₄] (9.2 mg, 10 μmol in 50 mL of toluene) were made up. Toluene (225 mL) was added to AlⁱBu₃ (1 M toluene solution, 5 mL, 5 mmol) and transferred to the reactor. The mixture was stirred for 5 min (1000 rpm) to “scrub” the apparatus. Ti(NⁱBu)(Me₃[9]aneN₃)Me₂ (1, 10 mL of stock solution, 2 μmol) was added to the reactor, followed by [Ph₃C][BAR^F₄] (10 mL of stock solution, 2 μmol). A dynamic ethylene pressure of 6 bar was applied. The temperature and ethylene uptake were monitored, and the reaction was run for 20 min, after which the ethylene flow was stopped and the pressure

carefully released. The reactor was opened and the reaction mixture “quenched” by careful dropwise addition of MeOH (ca. 10 mL). Distilled water (50 mL) was then added and the mixture acidified to pH 1 (10% HCl in MeOH) (ca. 25 cm³). The reaction mixture was stirred for 16 h and then filtered. The solid PE was washed with distilled water (1000 mL) and dried at ca. 100 °C to constant weight.

Ti(NⁱBu)(Me₃[9]aneN₃)Me(μ-Me)AlⁱBu₃ (1·TIBA). To a solution of Ti(NⁱBu)(Me₃[9]aneN₃)Me₂ (1, 7.0 mg, 0.022 mmol) in either C₆D₆ or C₆D₅Br (0.75 mL) was added a solution of AlⁱBu₃ (1.0 M in toluene, 21.9 μL, 0.022 mmol). A ¹H NMR spectrum recorded after 10 min contained resonances attributed to Ti(NⁱBu)(Me₃[9]aneN₃)Me(μ-Me)AlⁱBu₃ (1·TIBA). All other NMR tube reactions of metal dialkyl or monoalkyl cations were performed in an analogous way. ¹H NMR (C₆D₅Br, 499.9 MHz, 293 K): 2.76–2.59 (4H, overlapping m, NCH₂), 2.46 (6H, s, NMe *cis*), 2.25–1.82 (11H, overlapping m, NCH₂ and CHMe₂), 2.09 (3H, s, NMe *trans*), 1.09 (18H, d, ³J 6.5 Hz, CHMe₂), 1.07 (9H, s, NCMe₃), 0.14 (6H, d, ³J 7.0 Hz, CH₂CHMe₂), 0.06 (6H, br s, TiMe).

Crystal Structure Determinations of Ti(NR)(Me₃[9]aneN₃)Me₂·xC₆H₆ (R = ⁱBu (1·C₆H₆), ⁱPr (6·0.5C₆H₆), Ph (7), C₆H₃(CF₃)₂ (8), 2,6-C₆H₃ⁱPr₂ (9), 2-C₆H₄ⁱBu (11)) and [Ti(NPh)(Me₃[9]aneN₃){MeC(NⁱPr)₂}] [BAR^F₄]·CH₂Cl₂ (15-BAR^F₄·CH₂Cl₂). Crystal data collection and processing parameters are given in Tables 4 and 5. Crystals were mounted on glass fibers using perfluoropolyether oil and cooled rapidly in a stream of cold N₂

using an Oxford Cryosystems Cryostream unit. Diffraction data were measured using either an Enraf-Nonius KappaCCD diffractometer. As appropriate, absorption and decay corrections were applied to the data and equivalent reflections merged.⁹³ The structures were solved by direct methods (SIR92⁹⁴), and further refinements and all other crystallographic calculations were performed using the CRYSTALS program suite.⁹⁵ Details of the structure solution and refinements are given in the Supporting Information (CIF data). A full listing of atomic coordinates, bond lengths and angles, and displacement parameters for all the structures have been deposited at the Cambridge Crystallographic Data Centre. See Notice to Authors, Issue No. 1.

Computational Details. All the calculations have been performed with the Gaussian03 package⁹⁶ at the B3PW91 level.^{97,98} The titanium atom was represented by the relativistic effective core potential (RECP) from the Stuttgart group (12 valence electrons) and its associated basis set,⁹⁹ augmented by an f polarization function ($\alpha = 0.869$).¹⁰⁰ The remaining atoms (C, H, N, Al) were represented by a 6-31G(d,p) basis set.¹⁰¹ Full optimizations of geometry without any constraint were performed, followed by analytical computation of the Hessian matrix to confirm the nature of the located extrema as minima on the potential energy surface.

Acknowledgment. We thank the EPSRC, CNRS, and the British Council for support, Dr. S. R. Dubberley for collecting

(93) Otwinowski, Z.; Minor, W. *Processing of X-ray Diffraction Data Collected in Oscillation Mode*; Academic Press: New York, 1997.

(94) Altomare, A.; Casciaro, G.; Giacovazzo, G.; Guagliardi, A.; Burla, M. C.; Polidori, G.; Camalli, M. *J. Appl. Crystallogr.* **1994**, *27*, 435.

(95) Betteridge, P. W.; Cooper, J. R.; Cooper, R. I.; Prout, K.; Watkin, D. J. *J. Appl. Crystallogr.* **2003**, *36*, 1487.

the X-ray data for **6·0.5C₆H₆**, and DSM Research for generous gifts of [Ph₃C][BARF₄].

Supporting Information Available: X-ray crystallographic data in CIF format for the structure determinations of **1·C₆H₆**, **6·0.5C₆H₆**, **7**, **8**, **9**, **11**, and **15-BARF₄·CH₂Cl₂**. This information is available free of charge via the Internet at <http://pubs.acs.org>.

OM0606136

(96) Frisch, M. J.; Trucks, G. W.; Schlegel, H. B.; Scuseria, G. E.; Robb, M. A.; Cheeseman, J. R.; Montgomery, J. J. A.; Vreven, T.; Kudin, K. N.; Burant, J. C.; Millam, J. M.; Iyengar, S. S.; Tomasi, J.; Barone, V.; Mennucci, B.; Cossi, M.; Scalmani, G.; Rega, N.; Petersson, G. A.; Nakatsuji, H.; Hada, M.; Ehara, M.; Toyota, K.; Fukuda, R.; Hasegawa, J.; Ishida, M.; Nakajima, T.; Honda, Y.; Kitao, O.; Nakai, H.; Klene, M.; Li, X.; Knox, J. E.; Hratchian, H. P.; Cross, J. B.; Bakken, V.; Adamo, C.; Jaramillo, J.; Gomperts, R.; Stratmann, R. E.; Yazyev, O.; Austin, A. J.; Cammi, R.; Pomelli, C.; Ochterski, J. W.; Ayala, P. Y.; Morokuma, K.; Voth, G. A.; Salvador, P.; Dannenberg, J. J.; Zakrzewski, V. G.; Dapprich, S.; Daniels, A. D.; Strain, M. C.; Farkas, O.; Malick, D. K.; Rabuck, A. D.; Raghavachari, K.; Foresman, J. B.; Ortiz, J. V.; Cui, Q.; Baboul, A. G.; Clifford, S.; Cioslowski, J.; Stefanov, B. B.; Liu, G.; Liashenko, A.; Piskorz, P.; Komaromi, I.; Martin, R. L.; Fox, D. J.; Keith, T.; Al-Laham, M. A.; Peng, C. Y.; Nanayakkara, A.; Challacombe, M.; Gill, P. M. W.; Johnson, B.; Chen, W.; Wong, M. W.; Gonzalez, C.; Pople, J. A. *Gaussian 03*, Revision C.02; Gaussian, Inc.: Wallingford, CT, 2004.

(97) Becke, A. D. *J. Chem. Phys.* **1993**, *98*, 5648.

(98) Perdew, J. P.; Wang, Y. *Phys. Rev. B* **1992**, *45*, 13244.

(99) Andrae, D.; Haussermann, U.; Dolg, M.; Stoll, H.; Preuss, H. *Theor. Chim. Acta* **1990**, *77*, 123.

(100) Ehlers, A. W.; Bohme, M.; Dapprich, S.; Gobbi, A.; Hollwarth, A.; Jonas, V.; Kohler, K. F.; Stegmann, R.; Veldkamp, A.; Frenking, G. *Chem. Phys. Lett.* **1993**, *208*, 111.

(101) Hariharan, P. C.; Pople, J. A. *Theor. Chim. Acta* **1973**, *28*, 213.